Lehrstuhl für Computergestützte Modellierung und Simulation
Department of Civil, Geo and Environmental Engineering
Technical University of Munich

Continuous monitoring of construction site progress and activities with LIDAR-sensors

Scientific work to obtain the degree

Bachelor of Science (B.Sc.)

at the Department of Civil, Geo and Environmental Engineering of the Technical University of Munich.

Supervised by Prof. Dr.-Ing. André Borrmann
M.Sc. Fabian Pfitzner
M.Sc. Fiona Collins
Lehrstuhl für Computergestützte Modellierung und Simulation

Submitted by Jakob Fuchs [redacted]

Submitted on 17. March 2023

Acknowledgements

Foremost, I want to thank my supervisors and the Chair of Computational Modeling and Simulation for their trust and support during this work.
Additionally, I want to give a special thanks to Andreas Pürgstaller and Bergmeister Ingenieure GmbH for providing a digital building model. Furthermore, a special thanks to Innovationsmanagement Bau GmbH and Dipl.-Ing. Emil Hönninger GmbH & Co. Bauunternehmung KG for allowing access and providing support on their construction site.

Abstract

Digitalization in the construction industry enables the use of automatic monitoring with different data acquisition methods compared to manual traditional monitoring approaches. In current research, 3D point cloud data is mainly acquired by imaging technologies, such as image reconstruction or TLS. To overcome limitations by these technologies, we introduce acquisition of 3D point cloud data on construction sites using LIDAR sensors mounted on cranes. This work is split into a simulation and case study to determining a suitable sensor position and to collect scans over several time periods on a real construction site. Based on a BIM of the real construction site and properties of the Blickfeld Cube 1 Outdoor LIDAR sensor used in this work, we found a suitable scanner position near the crane's cabin to maximize the covered area. An evaluation of 221 scans acquired in the case study shows the importance of a compromise between the scan interval and scanner position, which is affected by crane's rotation limiting the ability to capture specific areas of the constructions site consistently. The LIDAR sensor used in the case study provides sufficient detail and quality to visually derive progress, showing the potential for automatic construction monitoring use cases.

Zusammenfassung

Die Digitalisierung in der Bauindustrie ermöglicht automatische Bauüberwachung mittels unterschiedlicher Methoden zur Datenerhebung im Vergleich zu traditionellen und manuellen Vorgehensweisen. In der aktuellen Forschung werden 3D Punktwolken hauptsächlich durch die Rekonstruktion von Bildern oder durch terrestrisches Laserscanning erhoben. Um die Einschränkungen dieser Technologien zu bewältigen, schlagen wir vor, 3D Punkwolken auf Baustellen mit LIDAR Sensoren auf Kränen zu erfassen. Dafür teilen wir diese Arbeit auf, in eine Simulation zur Bestimmung einer geeigneten Position eines Sensors und eine Fallstudie um Daten in mehreren Zeiträumen auf einer echten Baustelle zu sammeln. Basierend auf einem BIM der echten Baustelle und Eigenschaften des Blickfeld Cube 1 Ourdoor LIDAR Sensor, der in dieser Arbeit verwendet wird, konnte eine geeignete Sensor Position nahe der Krankabine ermittelt werden, um die abgedeckte Fläche zu maximieren. Die Auswertung von 221 Scans aus der Fallstudie zeigt die Relevanz eines Kompromisses zwischen dem Zeitintervall zwischen Scans und der Sensor Position, die durch die Rotation des Krans beeinflusst wird und ein konsistentes Erfassen bestimmter Regionen auf der Baustelle limitiert. Der LIDAR Sensor aus der Fallstudie ermöglicht ein ausreichendes Detailgrad und Qualität um Baufortschritt visuell nachvollziehen zu können, was das Potential für einen Einsatz in der automatischen Baufortschrittsüberwachung zeigt.

Contents

List of Figures

List of Tables

List of Algorithms

Acronyms

AEC	Architecture, Engineering and Construction
ALS	Aerial Laser Scanning
BIM	Building Information Modeling
FOV	Field of View
GPS	Global Positioning System
HVAC	Heating, Ventilation and Air Conditioning
ICP	Iterative Closest Point
IFC	Industry Foundation Classes
LIDAR	Light Detection And Ranging
MLS	Mobile Laser Scanning
PoE	Power over Ethernet
RFID	Radio Frequency Identification
TLS	Terrestrial Laser Scanning
UAV	Unmanned Aerial Vehicle
VPN	Virtual Private Network
XML	Extensible Markup Language

Chapter 1

Introduction

Digitalization in the Architecture, Engineering and Construction (AEC) industry affects the approach during many states of a building such as planning, construction and maintenance. Building Information Modeling (BIM) plays a major role in this development. Using BIM, we can represent a building with all of its components, such as structural elements or Heating, Ventilation and Air Conditioning (HVAC) systems, digitally. The digital representation of a building can be used during development, construction and operation (BORRMANN et al., 2018). Models created in the planning phase are often referred as a digital twin of a building (SACKS et al., 2020). However, changes and deviations during construction are not taken into account of as-planned models (SACKS et al., 2020). SACKS et al. (2020) emphasize that as-planned BIMs do not contain the actual physical state of a building during or after construction and are therefore not a digital twin of the real construction site. Capturing the as-built state of a construction site digitally is advantageous to keep track of a changing construction environment and helps managers to make effective informed decisions (SACKS et al., 2020).

Keeping track of an as-built model during construction requires continuous data from monitoring a constructions site. Collecting data manually is a labour intensive, error prone and time consuming task (SACKS et al., 2020). Therefore, different automatic data acquisition technologies are used on construction sites, such as laser scanning and computer vision (SACKS et al., 2020). In an approach to continuously collect data from construction sites, COLLINS et al. (2022) propose a workflow implementing cameras on cranes to monitor shell construction. While linkage from acquired data to building elements is possible, limitations arise from limited view-angles and overlap impeding photogrammetric reconstruction (COLLINS et al., 2022). These limitations raise the question, whether laser scanners on cranes are a viable approach to continuously acquire point cloud data on construction sites. Due to the high cost cost Terrestrial Laser Scanning (TLS), we focus on more affordable Light Detection And Ranging (LIDAR) sensors, which are typically used on mobile platforms (RAJ et al., 2020; TANG et al., 2022).

In this work, we use the LIDAR sensor 'Blickfeld 1 Cube Outdoor' ("Blickfeld", 2022), mounted on a crane on a real construction site to continuously acquire and analyse point cloud data over multiple time periods in a case study. After manually picking position candidates for the LIDAR sensor on a crane, based on the as-planned BIM of the real construction site, we carry out a simulation to determine a suitable sensor position based on the covered area by the sensor's limited Field of View (FOV) and occlusions. By analysing real world scans from the case study based on aspects such as the ability to derive progress and severity of noise and outliers, we discuss the viability of using LIDAR for continuous construction site monitoring.

In the context of construction monitoring, we first review the state of the art of commonly used data acquisition technologies and construction monitoring approaches in chapter 2. We then introduce our methodology in chapter 3, which is split up into a simulation to determine a suitable LIDAR sensor position and a case study deploying the sensor on a real construction site's crane in chapter 4 and chapter 5 respectively. Lastly, after reviewing the results of the case study, we discuss the challenges and viability of using LIDAR for continuous construction monitoring in chapter 6.

Chapter 2

State of the art

Continuously monitoring construction site progress requires continuous as-built data of the monitored building to be compared to as-planned digital building models. In this chapter, we discuss various data acquisition technologies used in construction. We then specifically focus on monitoring approaches using point clouds acquired by image reconstruction and laser scanning.

2.1 As-planned and as-built building models

Digital building models generally fall into the categories of as-planned and as-built models. These model categories are created in different project phases and require a different approach during creation. As-planned models contain a building in its intended shape and properties which are defined in the planning phase by architects and engineers. In the model's creation process, the building's attributes are fed into BIM software manually. During construction, digital building models are mainly used for collision detection and site logistics organization, which is enabled by using 4D BIM, containing additional schedule information (BORRMANN et al., 2018). After construction during building operation, models can be handed over to the owner, assisting facility and management systems (BORRMANN et al., 2018). However, as-planned models do not show the actual as-built state of a building, as they are not updated during construction (SACKS et al., 2020). Therefore, deviations or inaccuracies resulting from construction errors are not visible in as-planned models.

Models that show a building's actual state in the real world are as-built models. As-built models deviate from the as-planned models, from which their real world version was built from, due to inaccuracies or deviations during construction, changes after construction or renovations (DORE & MURPHY, 2014). Creating as-built models requires data acquisition on the construction site, which is discussed in the next section.

2.2 Construction monitoring

Limiting the cost of construction is of great interest for both contractors and clients. Enabling the detection of errors to reduce cost and schedule overruns on construction sites requires monitoring efforts (XUE et al., 2021). Traditionally, on-site monitoring is performed by manual visual and paper-based observations to keep track of progress, equipment, material, safety and schedule, which is labour-intensive and error-prone

(PUČKO et al., 2018; XUE et al., 2021). These challenges posed by manual monitoring result in less frequent monitoring on the construction site than required (XUE et al., 2021). Furthermore, traditional paper-based monitoring surveys are challenging to understand, as the surveys can only show real-world problems in an abstracted way using text and graphics (XUE et al., 2021). Therefore, the available time for efficient decision making that is needed to keep a project on schedule might not be sufficient, resulting in delays (JIANG et al., 2022).

2.2.1 Automated construction monitoring

To overcome the issues of traditional construction monitoring, many automated monitoring technologies are proposed in research. In construction, data is commonly acquired Enhanced IT, Geo-spatial technologies and Imaging technologies (OMAR & NEHDI, 2016).

Enhanced IT, such as multimedia and email services, are useful for improving communication between construction workers, while being cheap and easy to use (OMAR & NEHDI, 2016). These technologies have great potential for controlling delays and cost overruns, but can not provide metrics for assessing data collection for progress tracking (OMAR & NEHDI, 2016). While these technologies are being used on construction sites today requiring little training, Enhanced IT is limited to manual construction progress tracking (OMAR & NEHDI, 2016).

Geospatial technologies like Barcoding, Global Positioning System (GPS) and acRFID are used to track and identify objects (OMAR & NEHDI, 2016). For example, Radio Frequency Identification (RFID) uses tags attached to objects that can be read and written to (OMAR & NEHDI, 2016). As more tags require more maintenance, scalability is limited by increased cost (OMAR & NEHDI, 2016). OMAR and NEHDI (2016) concluded, that the main use for geospatial technologies is real-time material tracking in applications such as preconstruction management and resource management.

2.2.2 Imaging technologies

The previously mentioned technologies are mainly used to improve communication and monitor individual objects but they can not provide 3D information about the geometry and orientation of one or multiple building elements, which is advantageous for progress monitoring approaches in order to detect a correlation between acquired data and as-planned models. For the task of 3D data acquisition, imaging technologies such as image reconstruction and laser scanning are used on construction sites, producing point clouds of their environment (OMAR & NEHDI, 2016). Both image reconstruction and laser scanning use different approaches to generate point clouds and are discussed next.

2.2.3 Image reconstruction

Various low-cost and portable devices are able to capture images on construction sites today. HAN and GOLPARVAR-FARD (2017) mention an exponential growth of images and videos that are taken on construction sites due to recent developments of consumer devices with built-in cameras. Images are not only a useful visualization tool, but can also be used to generate point clouds algorithmically using photogrammetry (XUE et al., 2021). Different approaches are used to extract 3D information from images, depending on the availability of the camera's extrinsic and intrinsic parameters (COLLINS et al., 2022). XUE et al. (2021) discuss the use of fixed cameras with known parameters, whose images can be registered to a BIM by rotating and scaling. In this case, finding suitable camera positions is a challenge, since stable objects are required for cameras to be placed on, preventing changes to the camera's position and viewing direction (XUE et al., 2021). Additionally, the view of a fixed camera is prone to being occluded and full coverage of any object can only be ensured by increasing the number of cameras shooting from different directions (XUE et al., 2021). Alternatively, point clouds can also be generated from images without requiring extrinsic and intrinsic parameters. By matching unique feature points found by specialized algorithms in each image taken from different views, matching images with overlapping regions can be found to extract 3D information using triangulation (COLLINS et al., 2022).

2.2.4 Laser scanning

In the AEC industry, TLS is receiving increasing interest in recent years (WU et al., 2022). A study by WU et al. (2022) concluded five main applications of TLS by analysing related research publications of the last decade: 3D model reconstruction, object recognition, deformation measurement, quality assessment, and progress tracking. More specifically in context of building life cycles, TLS has become the main data source for BIM (LIU et al., 2021).

Opposed to indirectly reconstructing point clouds from images requiring algorithms, laser scanners directly acquire point clouds. TLS typically use time-of-flight or phase-based laser rangers to measure the distance from the scanner to objects (WU et al., 2022). 3D coordinates for each point are calculated by the measured distance S, the horizontal angle α and vertical angle β of the light emitting from the scanner, as shown in eq. (2.1) (WU et al., 2022).

$$\begin{pmatrix} X_p \\ Y_p \\ Z_p \end{pmatrix} = \begin{pmatrix} S\cos\beta\cos\alpha \\ S\cos\beta\sin\alpha \\ S\cos\beta \end{pmatrix} \tag{2.1}$$

TLS are usually capable of scanning within a large field of view, since they are capable of rotating 360° horizontally on a tripod. An additional vertically rotating mirror is used for deflecting laser beams vertically to expand coverage to 3D. Modern TLS are highly

accurate and scan points with up to 2 MHz, creating dense point clouds (HOLST et al., 2015). However, state of the art TLS equipment is expensive, easily surpassing 50.000 USD per scanner (TANG et al., 2022). Therefore, implementing TLS for a continuous monitoring use case yields highly detailed point clouds of a construction site, but requires significant expenses, especially when using multiple scanners for larger construction sites and during long time periods.

Laser scanning is not limited to TLS. In the AEC industry, Mobile Laser Scanning (MLS) and Aerial Laser Scanning (ALS), typically used by being mounted on mobile platforms like cars and Unmanned Aerial Vehicles (UAVs) are advantageous for special use cases covering large areas (WU et al., 2022). WU et al. (2022) compile common methods to acquire point clouds in the AEC industry including their general properties, as shown in table 2.1.

Table 2.1: Comparison of different point clouds acquisition methods (WU et al., 2022)

Technology	Tools	Range (In General)	Accuracy (In General)	Cost (In General)
Laser scanning	TLS	Moderate	0.5-10 mm	High
	ALS	Long	>10 mm	High
	MLS	Moderate	>10 mm	High
Photogrammetry	Smartphone-based	Close	>10 mm	Low
	UAV-based	Moderate	>10 mm	Moderate
Videogrammetry	Smartphone-based	Close	>10 mm	Low

In addition to these technologies, other LIDAR based methods able to acquire point clouds using time of flight measurements with reduced cost, size and weight are available today (RAJ et al., 2020). These devices use different scanning mechanisms specializing on various use cases (RAJ et al., 2020). (RAJ et al., 2020) mention an increased use of LIDAR on mobile platforms addressing problems such as obstacle avoidance, due to its light weight and small size. However, in the context of construction monitoring, little use of this maturing technology can be seen. Research focusing on data acquisition technologies for construction monitoring, such as OMAR and NEHDI (2016), does not differentiate laser scanning technologies and LIDAR and as such generally categorizes laser scanning as expensive, disregarding less costly LIDAR technologies. In more recent research, XU et al. (2021) mention the use of LIDAR as a customizable hardware system to capture 3D point clouds on construction sites, but still generally categorize laser scanning as expensive for 'satisfactory accuracy' (XU et al., 2021).

2.3 Automated progress monitoring

As previously mentioned, monitoring construction progress is essential to reduce cost and schedule overruns. Therefore, it is advantageous to automate this task to reduce time spent on manual labour intensive monitoring. Automated progress monitoring approaches are based on comparing a building's as-built state to its as-planned model, also referred to

as Scan-vs-BIM (JIANG et al., 2022). In research, numerous approaches using different data acquisition technologies and algorithms to derive progress are being explored. In the scope of this work, we introduce common approaches used in research. Point cloud based approaches are mostly similarly structured and consist of data acquisition, registration and derivation of progress.

Generally, all cameras and laser scanners, independent of their quality, range or FOV are limited by occlusions. Static occlusions, caused by progress itself and temporary structures like scaffolding, and dynamic occlusions by machinery and workers impact the captured area during data acquisition (GOLPARVAR-FARD et al., 2015). Depending on the use case, different data acquisition methods are used, which are optimized for individual use cases. For example, JIANG et al. (2022) use two TLS to verify the volume of bridge elements during construction. Using two TLS gives the authors accurate and dense point clouds, but their scans are still severely limited by occlusions and registration issues requiring manual intervention.

The registration process is a cornerstone for methods comparing point clouds to a BIM, since no comparisons between arbitrarily oriented point clouds in the coordinate system of a BIM can be made. Therefore, during registration, point clouds are lined up with their corresponding as-planned BIM. In current research, different registration methods are used. Common registration approaches line up point clouds manually or by using an Iterative Closest Point (ICP) algorithm (BRAUN et al., 2020). ICP aligns BIM geometry and point clouds by minimizing the distances between points (BRAUN et al., 2020). However, KAVALIAUSKAS et al. (2022) note that a coarse registration is required before performing fine registration using ICP. A combination of manual coarse registration and fine registration using ICP is implemented by JIANG et al. (2022), requiring a manual selection of corresponding points in an as-built point cloud and as-planned model. KAVALIAUSKAS et al. (2022) use a different approach, in which they combine control points and an automatic positioning system integrated into a TLS, which requires control points in a line of sight to the scanner to be available.

After registration, a comparison between acquired point clouds and a corresponding BIM can be performed. However, the question arises how a direct comparison can be made, since point clouds and BIMs are different file formats and represent 3D information differently (KAVALIAUSKAS et al., 2022). BRAUN et al. (2020) point out two different approaches to compare point cloud data to a BIM. First, the registered as-built point cloud can be compared to a BIM sampled as a point cloud (BRAUN et al., 2020). In this approach, the geometry of BIM objects is sampled to an as-planned point cloud, allowing detection of building elements using point proximity metrics (BRAUN et al., 2020). Second, the as-built point cloud and triangulated BIM geometry surfaces can be matched (BRAUN et al., 2020). KAVALIAUSKAS et al. (2022) use this method by extracting geometry from an Industry Foundation Classes (IFC) model to generate plane equations for each face in every building object. A threshold and plane limits then decide, whether points relate to an object, by checking the distance to each plane (KAVALIAUSKAS et al., 2022).

2.3.1 Continuous monitoring

Continuously monitoring a construction site further focuses on automating data acquisition. Research on continuous data acquisition in progress monitoring is rare, while the focus mainly lies on as-built data processing. COLLINS et al. (2022) emphasize the need for large-scale datasets generated automatically and steadily over time. Automatic data acquisition is an important step in progress monitoring, since sporadic and manual as-built data collection is not sufficient for steady construction monitoring (COLLINS et al., 2022).

Ensuring steady data acquisition raises the problem of finding suitable locations for data acquisition equipment such as laser scanners or cameras in order to cover specific areas of a construction site. This problem can be described by a trade-off between the number of data acquisition devices and the severity of occlusions limiting their view. The availability of suitable locations for cameras or laser scanners that have an unoccluded view onto a construction site differs, depending on requirements limiting possible positions and special mounting possibilities such as cranes or tall adjacent buildings. Continuous data acquisition is especially limited by dynamic and static occlusions (GOLPARVAR-FARD et al., 2015). While machinery and workers causing dynamic occlusions are natural on construction sites, static occlusions caused by construction progress itself can severely impact and block the view to large parts of a building (GOLPARVAR-FARD et al., 2015).

Capturing all building elements continuously is impractical, since indoor elements occluded by walls and ceilings require a large number of cameras or laser scanners to be fully covered. Therefore, acquiring point cloud data with optimized positions for camera and laser scanners to maximize the coverage of targeted building elements is essential, since most areas on constructions sites can be captured before being occluded by subsequent building progress.

However, the rate of data acquisition, defining how frequently images or scans are taken, must match the speed of construction. Fast construction progress achieved by prefabrication may occur between two scans, skipping the acquisition of building elements that may be occluded afterwards (GOLPARVAR-FARD et al., 2015). Especially on fast progressing construction sites, a trivial solution to this problem would require shorter scan intervals increasing data volume and processing efforts.

2.4 Contribution

In this work, we propose an approach to continuously acquire point cloud data using LIDAR sensors to monitor shell construction. Hereby, we contribute to state of the art approaches by

1. proposing the use of affordable LIDAR sensors on cranes to monitor construction site progress

2. introducing a workflow to obtain a suitable scanner position on cranes by using a simulation
3. acquiring a dataset of point clouds over multiple time periods from a scanner mounted on a crane on a real construction site
4. analysing our results emphasizing on the need of a compromise between scan frequency and the mobility of scanner positions

Chapter 3

Methodology

3.1 Data acquisition using LIDAR-scanners on construction sites

In the scope of this work, we focus on data acquisition using LIDAR sensors for continuous shell construction progress monitoring. We specifically limit our approach to scanning from cranes, utilizing elevated scanner positions to our advantage. In case of scanning construction sites from cranes, each individual building element is likely to be visible from the scanner, unless it is occluded by successive building elements, such as the floor of the next storey. Especially in shell construction, new building elements structurally rely on previously built elements. Therefore, the time frame varies, in which any building element is visible to the scanner until occluded by successive elements. Additionally, limiting our approach to shell construction enables us to capture the construction site with few occlusions caused by other trades, such as facades or drywalls.

Using LIDAR, geometric 3D point cloud data of the construction site can be acquired directly. Opposed to TLS, using LIDAR sensors is less expensive and enables easier portability due to smaller and lighter devices. In our use case, a limited FOV from a LIDAR sensor opposed to full 360° horizontal coverage with TLS is sufficient, since scans from cranes are only required to capture in the downwards direction. In comparison to using cameras for data acquisition, LIDAR scanners have the advantage of directly capturing their environment without requiring algorithms to reconstruct 3D data from images, requiring significant processing efforts (COLLINS et al., 2022).

3.2 Approach to analysing LIDAR-scanner capabilities

3.2.1 General procedure

To analyse the viability of LIDAR sensors for our use case, we propose a procedure consisting of a simulation and case study, as shown in fig. 3.1. This flowchart illustrates the procedure and is separated into requirements, workflow and discussion. The Requirements include essential devices and models, such as a BIM, a specific LIDAR sensor acting as the scanner and networking setup on the construction site that are needed before continuing with further steps.

First, a simulation is performed to find a suitable scanner position based on the scanner's specification and the building's geometry to monitor construction progress. Ideally, the

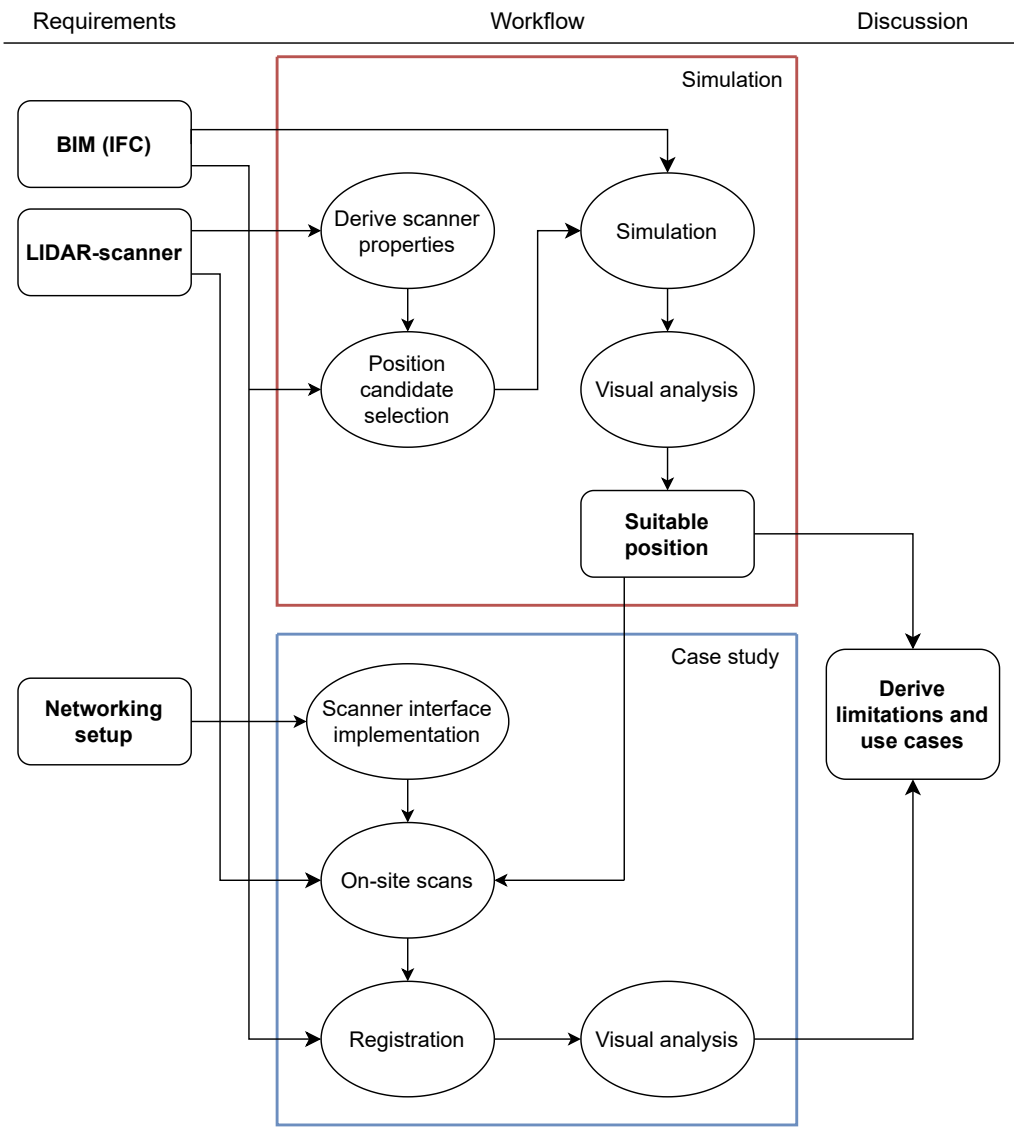

Figure 3.1: Required tasks for the methodology split into a simulation and case study

simulation uses a BIM of the monitored building from the case study and the real scanner's properties to generate realistic point clouds. To gain meaningful and rich information from scans, a suitable scanner position must be found. We examine the visible area of the construction site from different scanner positions on the crane in terms of size and occlusions. In the scope of this work, we manually analyse simulated point clouds for each position to determine a suitable position.

This approach is not limited to using one scanner, since multiple point clouds from simulated scans can be combined and are automatically registered. Registered point clouds of multiple scans enable the analysis for different scanner position combinations. While more scanners increase cost, data use, networking and synchronization efforts, a larger scanned area from different angles of the construction site can be achieved. In the scope of this work, we limit our approach to one scanner.

The position determined in the simulation for one or multiple scanners can then be used in the case study. To acquire predictable and comparable scan results in the case study, the

real scanner must be mounted using the position and orientation obtained in the simulation. A hardware and networking setup at the construction site and on the crane to store scans and offer remote control to allow on-demand access for scan data is required. Additionally, hardware at the construction site must be robust to withstand harmful outdoor conditions, potentially damaging electronic devices. Furthermore, a software interface capable of communicating with the scanner enabling the ability to send data from the scanner to an on-site computer must be implemented. Using adequate hardware and software, we can continuously collect, store and provide remote-access to data from the scanner on the construction site.

In a final step, we discuss acquired scans and the potential for continuous monitoring approaches. We visually derive limitations by manually registering point clouds from the case study with the BIM. Hereby, we examine the impact of real world factors, such as noise and crane rotation during operation. Our workflow ensures the use of LIDAR sensors on real construction sites to be based on data gained in simulations that can be verified in practice.

3.2.2 Scanner and model introduction

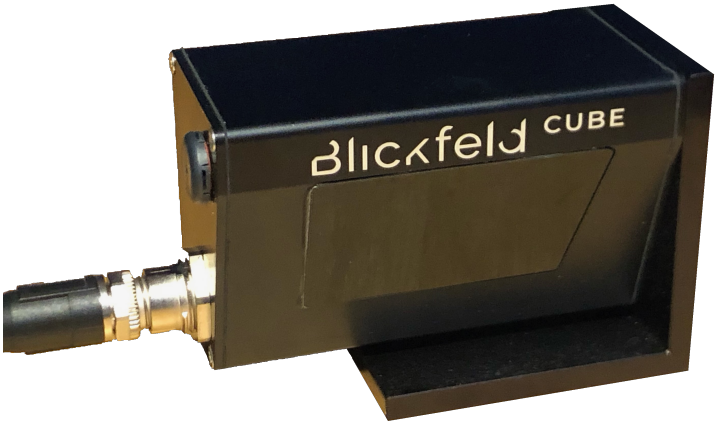

Figure 3.2: Blickfeld Cube 1 Outdoor LIDAR sensor

In the following chapters, we use the Blickfeld Cube 1 Outdoor, which is a solid-state 3D LIDAR sensor, shown in fig. 3.2 (“Blickfeld”, 2022). This LIDAR sensor is easily portable with a weight of 330 g and height, width and depth of 60 mm x 97 mm x 50 mm (“Blickfeld”, 2022). Additionally, the LIDAR sensor has an IP65 rating, which ensures outdoor usage and enables use on cranes (“Blickfeld”, 2022). In this work, we refer to the Blickfeld Cube 1 Outdoor as the ’scanner’.

The case study is performed using the scanner on a real construction site. We have access to an IFC model containing geometric information about all building elements for shell construction, shown in fig. 3.3, referred to as the BIM in this work. However, the IFC model has no reference to the construction schedule. Therefore, building models

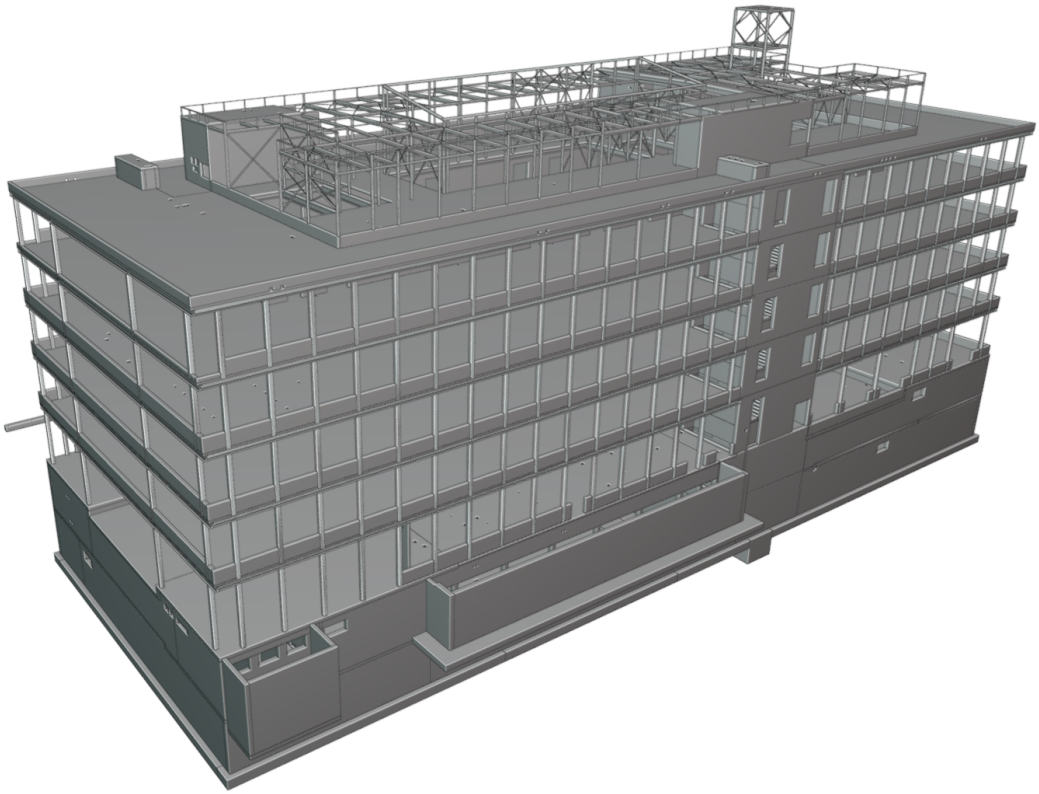

Figure 3.3: Complete IFC model of the building used in simulation and case study

with partly finished construction progress, used in the simulation and case study, must be manually created by trimming the original IFC model.

Chapter 4

Simulation

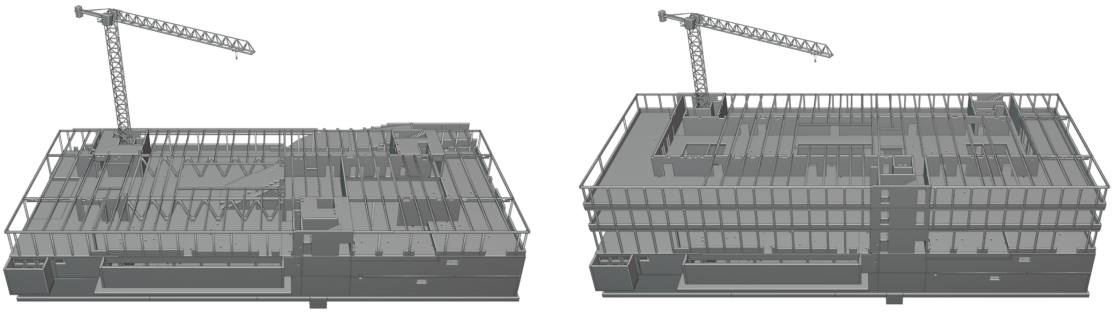

(a) Early construction progress

(b) Intermediate construction progress

Figure 4.1: Trimmed building models

In the simulation, we aim to find a suitable position on a crane for one scanner at the construction site of the case study. As a baseline for the simulation, we use manually trimmed IFC models using “BlenderBIM” (n.d.), based on the complete IFC model. The trimmed models represent the building during an early and intermediate state of construction, shown in fig. 4.1. In addition, the intermediate construction model is also an approximate model of the state of the real construction site when data acquisition is started for the case study, shown in fig. 4.1b. Therefore, simulated point clouds for this model are especially valuable for choosing a suitable scanner position that can later be used in the case study. Additionally, to improve visualization of scanner positions and orientations, a crane model is added to the actual location of the real crane on the constructions site in the elevator shaft. The simulation is based on scanner positions on the crane, whose top section is rotated towards the centre of the construction site, maximizing coverage of building elements.

4.1 Position candidates

Since we do not implement automatic metrics to evaluate simulated scans, we must manually select positions for the simulation on the crane. First, a set of position candidates from all possible mounting positions on the crane must be selected, which are further examined in the simulation. Position candidates are selected based on the scanner’s limited FOV and size of the captured area. Using the Blickfeld Cube 1 Outdoor, a maximum FOV of 70x30° horizontally and vertically is available (“Blickfeld”, 2022). Other scanner parameters affecting the point cloud density are not considered when choosing position

candidates, since the simulation software can not accurately replicate the scan pattern of the Blickfeld Cube 1 Outdoor.

When selecting position candidates, boundary conditions are set to limit selection possibilities for our use case. To ensure an optimal view of the scanner in the vicinity of the crane, we exclude all scanner positions on lower parts of the crane's tower. Since building progress surpasses these positions during construction, the scanner's view is mostly occluded, especially in our case when the crane is located in the elevator shaft and surrounded by the building. Therefore, we only consider elevated scanner positions, including positions close to the cabin and along the crane's jib to utilize the crane's height and length, maximizing the scanned area and enabling different angles to scan from. However from elevated positions, the scanner must be pitched downwards to keep the construction site in its FOV, posing a new problem of finding suitable pitch rotations. We expect that scanning downwards vertically results in less occlusions horizontally, but vertical elements such as walls or columns may not be recognizable due to the scanner not being able to reach their sides. In return, pitching the scanner horizontally increases the observed area but may cause horizontal occlusions. Therefore, it appears that an optimal pitch is dependant on the crane's height and building geometry.

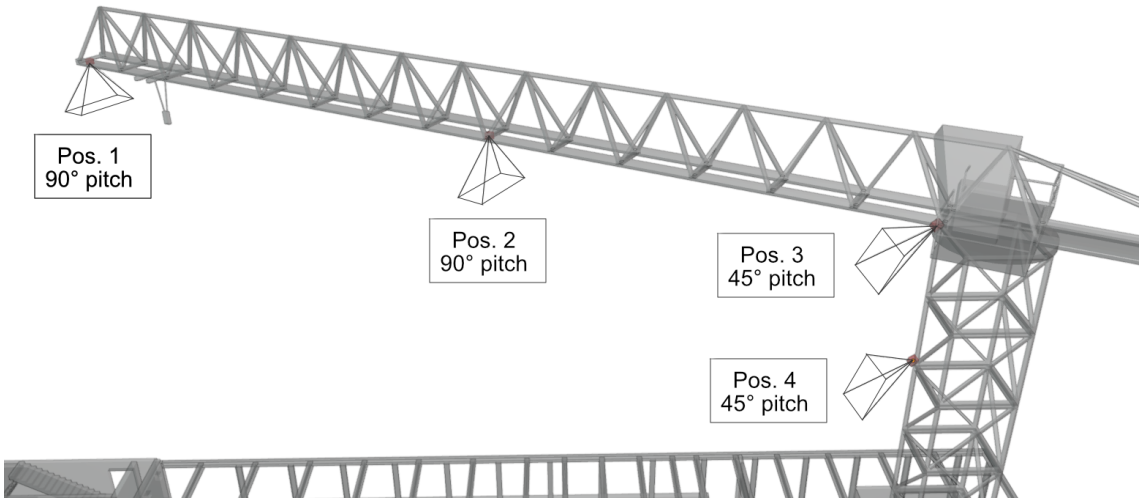

Figure 4.2: Scanner position candidates on the crane

Based on the boundary conditions for the scanner positions and limitations posed by the scanner's FOV, four position candidates are selected and further investigated in the simulation, shown in fig. 4.2. Position candidates 1 and 2 use a 90° downwards pitched scanner in the middle and at the end of the crane's jib. A pitch of 90° is necessary to ensure that the scanned area is within the crane's vicinity. By simulating scans from both positions, different areas of the construction site are captured. In our case, a rectangular recess in the floor of each storey is located below position 1. Position 3 and 4 use a 45° downwards pitched scanner located at different heights near the crane's tower. While position 3 is located on the crane's top section and would rotate during operation in practice, position 4 is located on the tower and does not rotate. Positions 3 and 4 selected to analyse the

influence of smaller changes in height on the scanned area for 45° downwards pitched scanners.

4.2 Simulation software

For the simulation, we use HELIOS++, a software package that is able to simulate TLS, MLS and ALS surveys (WINIWARTER et al., 2022). HELIOS++ allows a modular structure to configure simulations, which is required for our use case using different building models, scanner positions and scanner properties. A simulation can be customized by defining a survey that links to each of its components, such as the scanner, platform and scene (WINIWARTER et al., 2022). Components must be implemented using Extensible Markup Language (XML) files, allowing easy modifications (WINIWARTER et al., 2022).

4.3 Implementation

4.3.1 Simulation challenges

While HELIOS++ is capable of simulating different scan patterns that are commonly used in TLS, ALS and MLS, the scan pattern of the Blickfeld Cube 1 Outdoor is not supported. The Blickfeld Cube 1 Outdoor LIDAR sensor uses two oscillating MEMS mirrors in vertical and horizontal orientation to deflect laser beams in directions defined by the angle of both mirrors ("Scan pattern", n.d.). As the scan pattern is not supported by HELIOS++, we implement the simulation using the scan pattern of a TLS and limit the vertical and horizontal scan angles to replicate the Blickfeld Cube 1 Outdoor's FOV. Therefore, parameters affecting the point cloud density from the Blickfeld Cube 1 Outdoor can not be transferred into the simulation, since the simulation requires parameters specific to a TLS. As such, we neglect any scanner properties not linked to FOV, as data generated in the simulation would not be transferable to the case study.

In HELIOS++, the FOV for TLS can simply be modified by defining a range of vertical and horizontal angles. However, scanning downwards vertically requires a limited FOV beneath the scanner, which can not be achieved by limiting vertical and horizontal scan angles, as a the vertical scan angle exceeds -90°, which violates the maximum vertical scan angle of a TLS in HELIOS++. Therefore, a workaround for vertical downward scans is required.

To achieve a 70x30° FOV while facing downwards, the scanner generating a horizontal scan with the same FOV must be rotated 90° around the x-axis. However, HELIOS++ does not support rotation of static TLS. Therefore, scanner properties for the `headRotateAxis` and `beamOrigin` must modified as a workaround. To illustrate the required rotations, the local coordinate system of the scanner and a horizontal and vertical scan with a 70x30° FOV, simulated on a horizontal and vertical plane, are shown in fig. 4.3. Both simulated

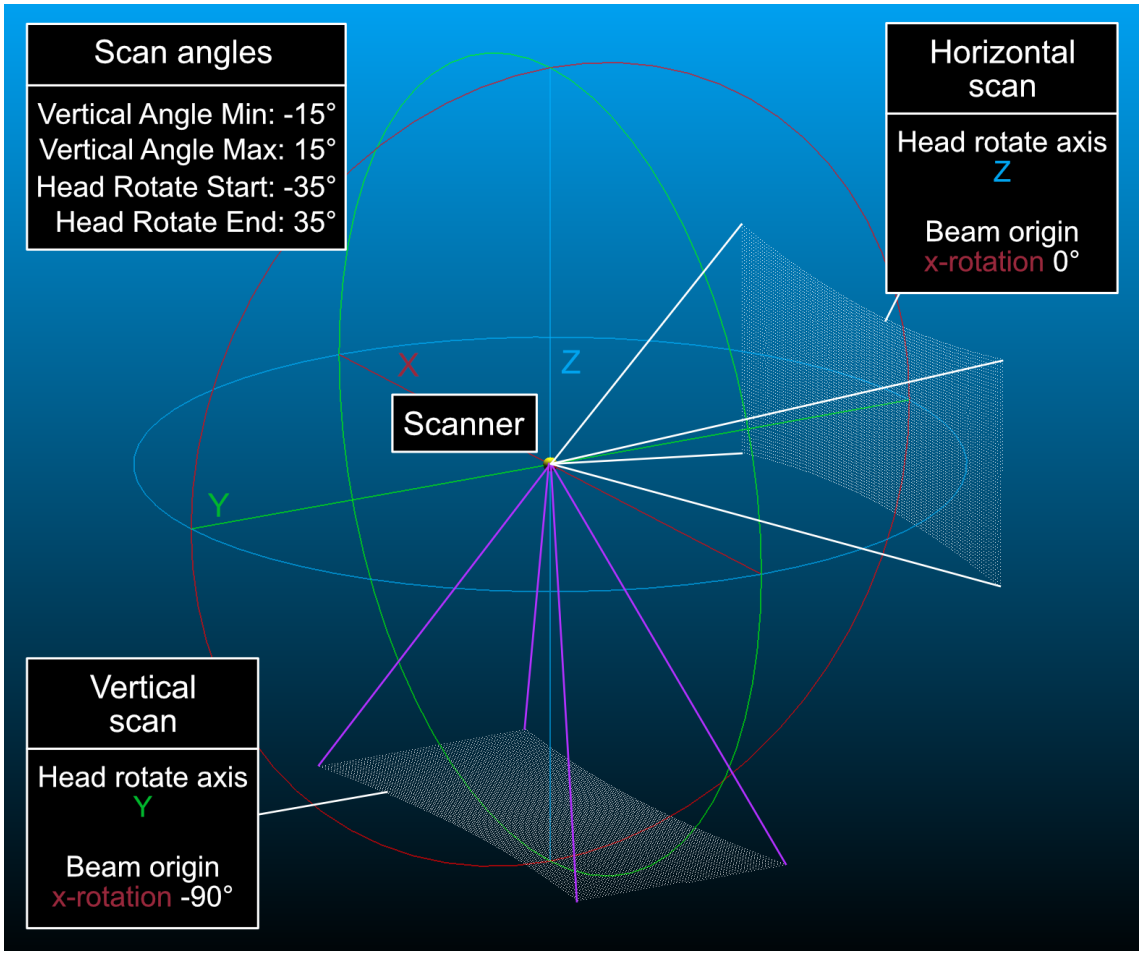

Figure 4.3: Simulated horizontal and vertical scan on flat planes, including scanner properties used in HELIOS++

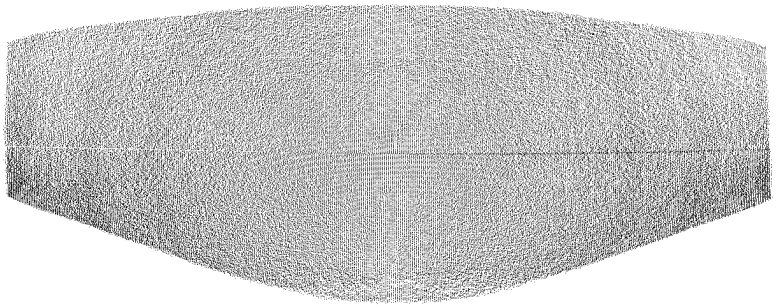

Figure 4.4: Top-down view on a real scan on a flat surface acquired with the Blickfeld Cube 1 Outdoor

scans are configured for a 70x30° FOV, by defining scan angle minima and maxima from -35° to 35° horizontally and -15° to 15° vertically, resulting in 70° and 30° respectively. By rotating the scanner head around its y-axis while rotating the beam Origin by -90° around the x-axis, a similar scan pattern to a horizontal scan can be achieved for a vertical scan. In comparison to the simulated scan, a real downwards scan acquired by using the Blickfeld Cube 1 Outdoor is shown in fig. 4.4. A different shape of the point cloud due to different scan patterns can be observed. To simulate -45° pitched scans, we use a

`headRotateAxis` around the z-axis and simply rotate the `beamOrigin` by -45°. Finally, to match the scanner with the rotation of the crane towards the centre of the construction site, an additional rotation of the `beamOrigin` by 30° around the y-axis is added.

4.3.2 Implementation of XML components

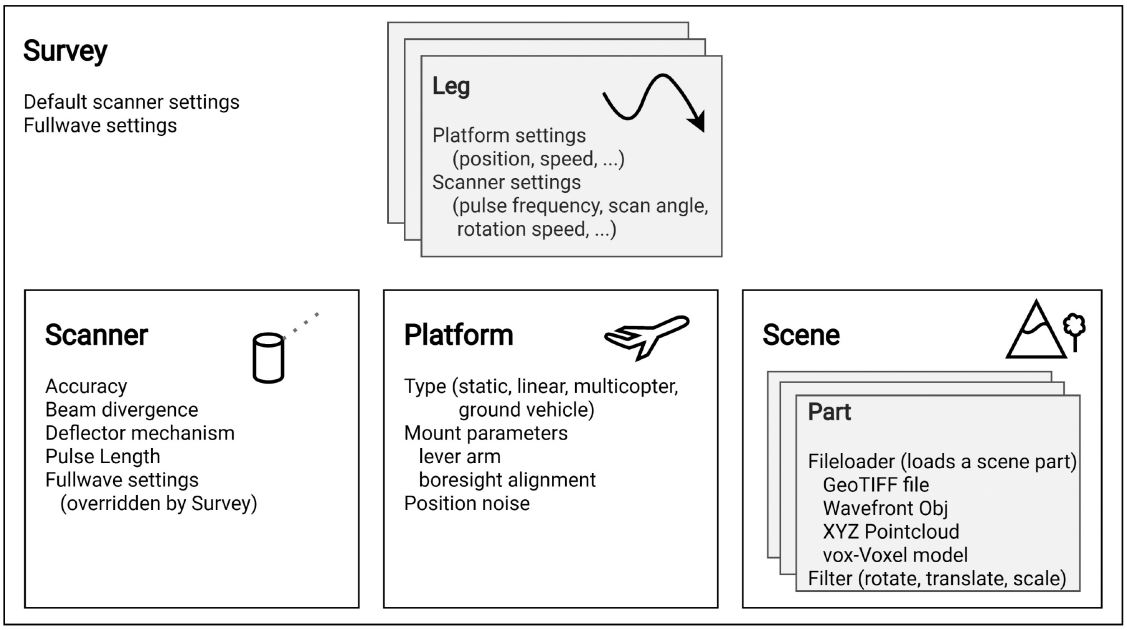

Figure 4.5: Components of a HELIOS++ survey. Source: WINIWARTER et al. (2022)

To simulate scans from the position candidates on both building models, we implement the required HELIOS++ components, shown in fig. 4.5, using XML. First, the required scanner components are built upon a TLS pre-set provided by HELIOS++. To achieve the required pitch rotations, we implement two individual scanners, one for a -45° and one for a -90° pitch, only modifying the parameters `beamOrigin` and `headRotateAxis` as previously discussed. For example, Algorithm 4.1 shows the implementation of modified scanner properties for a vertical downwards scan with a 30° rotation of the crane. Therefore,

Algorithm 4.1: XML implementation of scanner properties for a vertical downwards scan with a 30° crane rotation

```
<beamOrigin x="0" y="0" z="0.0">
        <rot axis="y" angle_deg="30" />
        <rot axis="z" angle_deg="0" />
        <rot axis="x" angle_deg="-90" />
</beamOrigin>
<headRotateAxis x="0" y="1" z="0"/>
```

scanner accuracy and point cloud density are based on a TLS in the simulation. Second, we define the platform component that specifies the scanner's mount. A static scanner mount with no offset is required, as the scanner's positions are specifically defined in the survey. Third, a scene must be defined to integrate each 3D model in the simulation. We specify the path to all 3D models using the wavefront (.obj) format and apply a translation

to position the models in the coordinate system of the simulation. To ensure support in HELIOS++, the trimmed IFC models of the building are converted from IFC to wavefront using “BlenderBIM” (n.d.). Finally, all scanner, platform and scene components are linked in surveys. Similar to the scanners, a survey for each pitch rotation is needed that refers to its corresponding scanner rotation. The surveys contain the scanner positions, specifying each position in a `leg`. Additionally, the vertical and horizontal scan angles of the scanner are defined in the survey. The XML files implementing the required components are included in appendix A.

4.4 Visual analysis of simulated scans

Running the simulation generates point clouds for each position and each building model for early and intermediate construction progress, shown in fig. 4.6 and fig. 4.7 respectively. Each figure contains two labeled scans with point clouds coloured in white and green, which are overlaid with the BIM. We analyse the results considering the covered area and limitations by occlusions. First, we can observe that the covered area in scans using the early construction building model is larger than in scans using the intermediate construction building model. Larger distances of the scanner to the building increase the covered area of scans, which is especially visible when comparing the coverage of horizontal beams from the BIM between position 1 in early and intermediate construction, shown as the white point clouds in fig. 4.6a and fig. 4.7a.

Independent of the building model, -90° pitched scans in positions 1 and 2 cover less area than -45° pitched scans, but are less impeded by occlusions from walls. As expected, -90° pitched scans barely depict the sides of horizontal structures such as walls and beams, when the scanner is located directly above. This can be observed in scanner position 2, in which walls not covered at all. However, in cases where walls have some distance horizontally to the scanner, a -90° pitched scan can also reach walls, as shown in position 1 in fig. 4.7a.

Especially for the BIM in our case, it is evident that depth information of lower floors is captured through the rectangular recess area in the center of the construction site in position 1 due to the vertical scanner orientation, shown in fig. 4.7a. Position 2 is limited to capturing one storey, as lower storeys are occluded by the upper most floor. In a direct comparison of the captured area between position 3 and 4, it is evident that position 3 covers an increased area and more distant elements due to the higher scanner position, shown in fig. 4.7b for positions 3 and 4.

As we use one scanner in the case study with the goal of obtaining large and diverse scan areas to analyse, position 3 is chosen. Positions 1 and 2 are ruled out due to the limited covered area in their scans and difficulty to set up the scanner on the crane’s jib in practice, requiring significant effort using climbing equipment. Position 1 provides detailed point clouds covering the recess through the floors of each storey in our case. However, we are interested in capturing each building element on the upper most storey.

In a comparison between positions 3 and 4, position 3 is chosen because of the larger and different areas that can be captured by mounting the scanner to the crane's rotating top section. The influence of crane rotation on scans is not considered in the simulation and must be analysed in the case study.

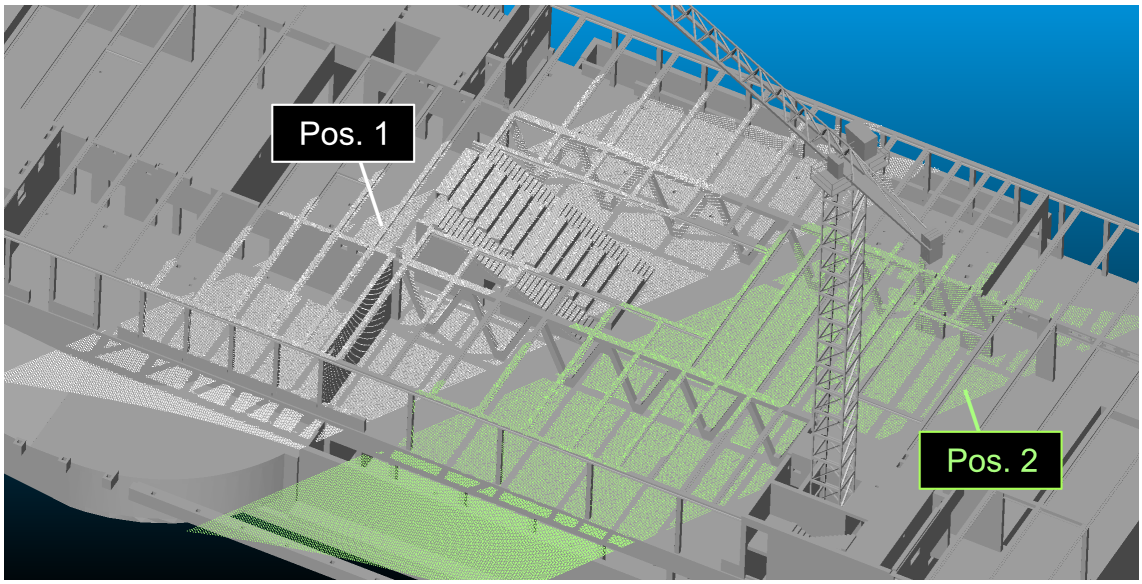

(a) Positions 1 and 2

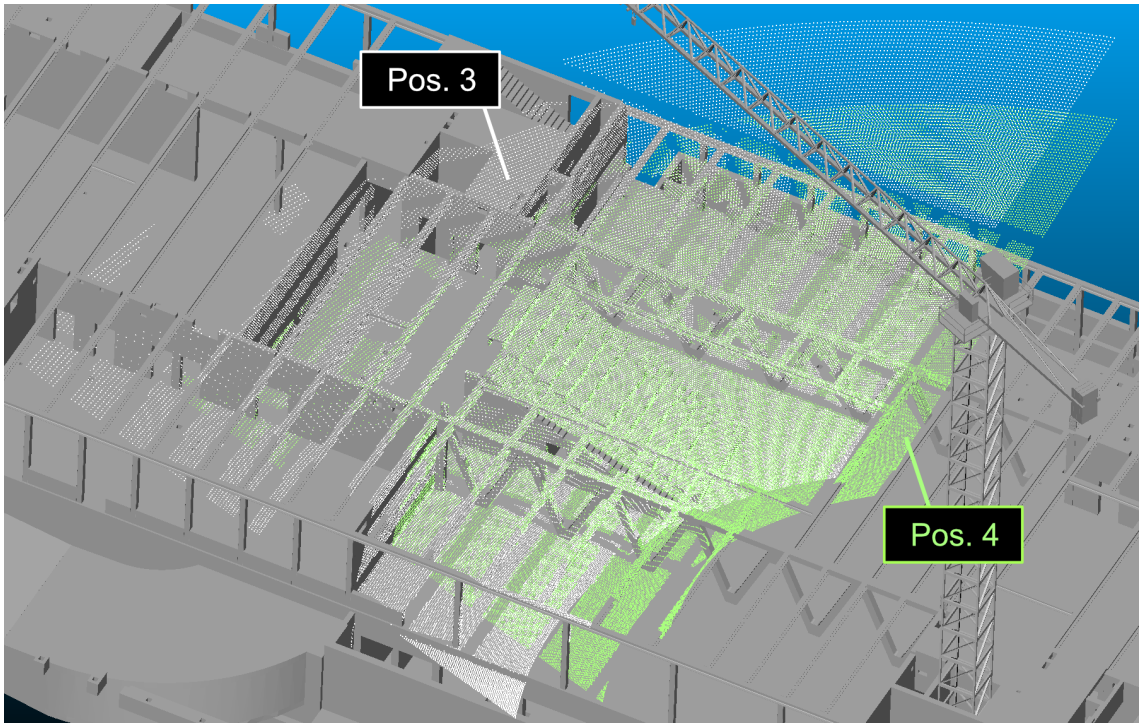

(b) Positions 3 and 4

Figure 4.6: Simulated point clouds on early construction progress building model

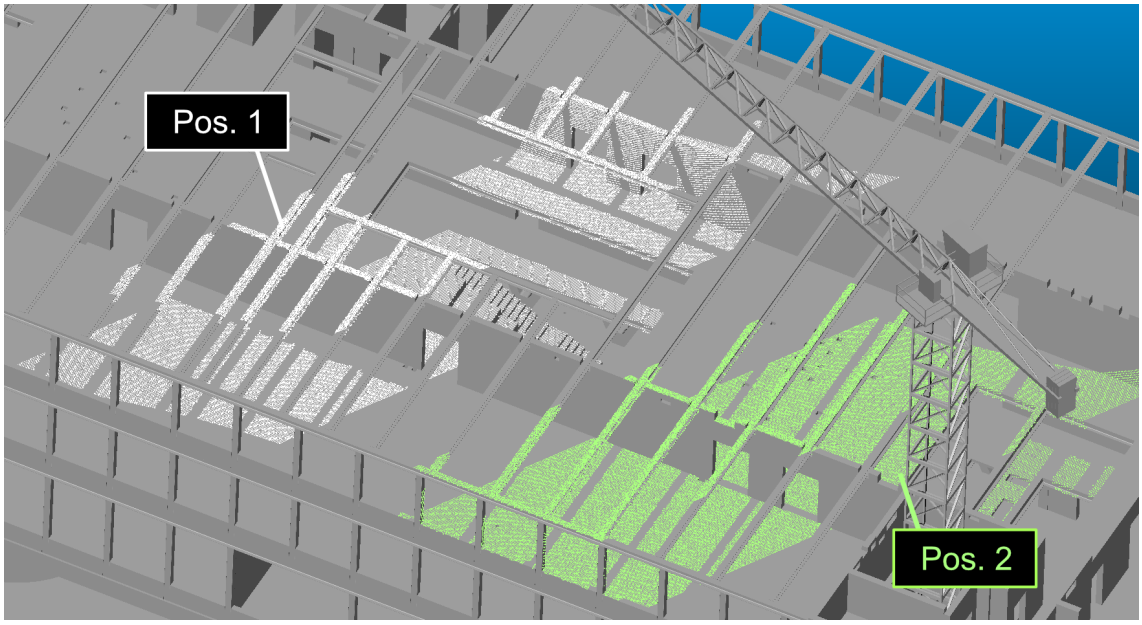

(a) Positions 1 and 2

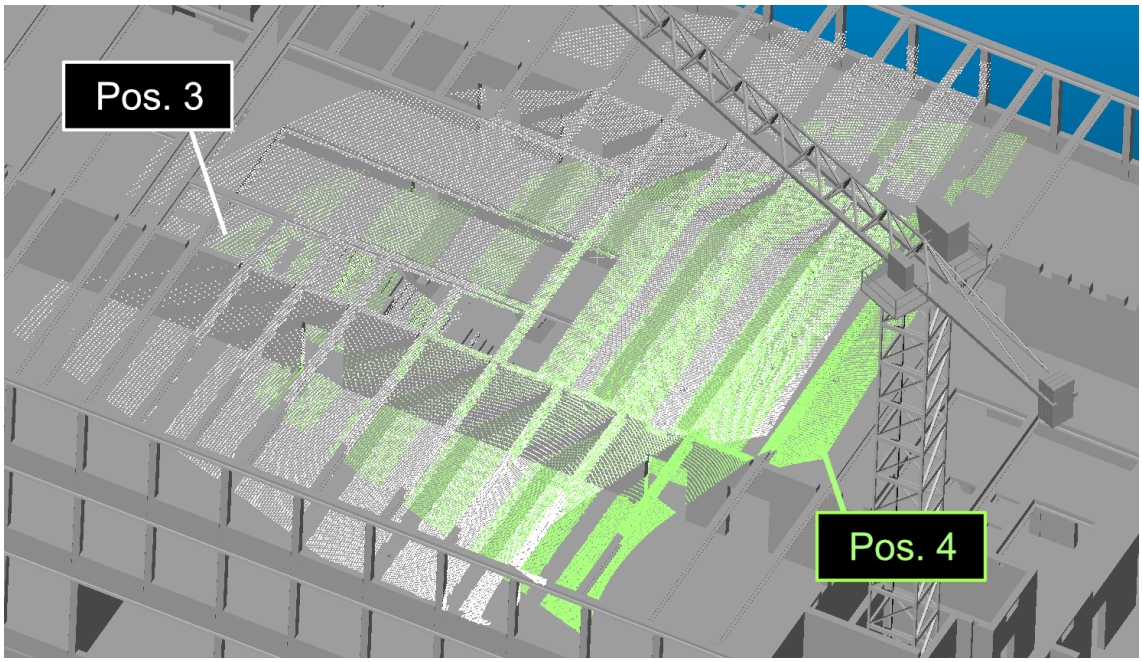

(b) Positions 3 and 4

Figure 4.7: Simulated point clouds on intermediate construction progress building model

Chapter 5

Case study

Figure 5.1: Scanner fixed to crane on real construction site

With the goal of analysing the viability of LIDAR sensors mounted on cranes in construction, we carry out a case study to acquire and examine real scan data over multiple time periods. Opposed to the simulation which generates point clouds for a specific state of construction for multiple scanner positions, we acquire real scan data from a single scanner position over time in the case study. With real data, we can further analyse the scanned area and occlusions by comparing scans from the case study and simulation. Additionally using real scans, we can analyse point cloud density and noise, which was not possible in the simulation, due to limitations of replicating the scan pattern and missing outdoor conditions.

Our methodology suggests simulating the scanner for different positions first, to obtain a suitable position for the real construction site before carrying out actual data acquisition. However, during testing on the construction site, the scanner was mounted on the crane next to the cabin, before performing the simulation, shown in fig. 5.1. Due to the advantages of position 3 established in the simulation, we were able to keep the scanner at the same position from testing, which approximately matches the position and orientation of position 3 in the simulation and acquire a larger dataset over a longer timespan.

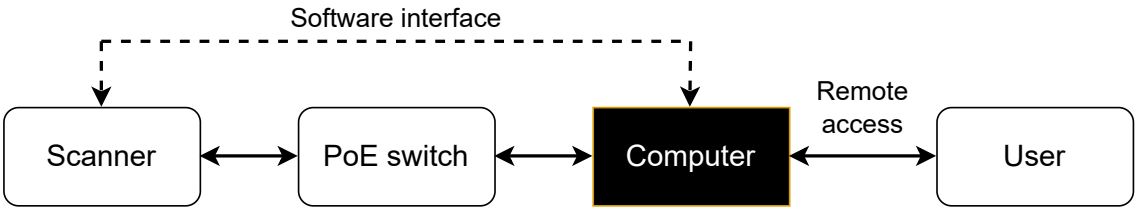

Figure 5.2: Hardware elements and scanner communication in case study

5.1 Hardware setup

Using the Blickfeld Cube 1 Outdoor as a standalone hardware device is not possible. A hardware setup with the means to communicate with the scanner and ability to provide remote access and local storage is required. Hardware Elements and the role of the software interface used in the case study are shown in fig. 5.2. The scanner receives power and transfers data using a single cable connected to a Power over Ethernet (PoE) switch. The PoE switch is connected to a computer that receives data from the scanner. A connection between the computer and scanner is managed by a Python software interface that schedules and saves scans. The computer is part of a collection of devices set up by COLLINS et al. (2022), who use it in a similar use case for storing and processing continuous images from cranes. Their setup includes a router, a Raspberry Pi connected to a Virtual Private Network (VPN) and a local server, contained in a water-proof box (COLLINS et al., 2022). In the scope of this work, we use these devices as a black box, to which we connect our scanner that is capable of communicating with the computer, storing data locally and providing remote access to data. More detail on the design choices of the computer and network are discussed in COLLINS et al. (2022).

5.2 Software interface implementation

Transferring data between the computer on the construction site and scanner is possible by using a software interface. To acquire continuous data in fixed time intervals, scans must be automatically scheduled. The Blickfeld Cube 1 Outdoor offers a web interface that is able to configure the scanner's scan pattern and run scans manually, which is not sufficient for continuous scans in our use case. We use the open source Python library `blickfeld_scanner`, provided by the scanner's manufacturers, to communicate with the scanner from the computer at the construction site (BLICKFELD, 2023). The library enables us to request scans from a Python script programmatically. Using the same Python script, scans can be further processed and saved on the local server.

Obtaining and processing raw data using the `blickfeld_scanner` library is handled by a `scan` function, shown in Algorithm 5.1. For each scan, we establish a new connection to the scanner by specifying its host name or IP address passed to the function by the `device` parameter. The connection automatically gets closed after exiting the scope of the function. Using the connection, we have access to a point cloud stream provided from the

Algorithm 5.1: Function to obtain a point cloud from a single scan

```python
def scan(device: str) -> List[List[float]]:
    points = []
    try:
        scanner = blickfeld_scanner.scanner(device)
    except Exception:
        print(f"Failed to connect to device: {device}")
        return points
    print(f"Connected to device {device}")
    stream = scanner.get_point_cloud_stream()
    print("Receiving frame...")
    frame = stream.recv_frame()
    print("...Frame received")
    for scanline in frame.scanlines:
        for point in scanline.points:
            for point_return in point.returns:
                x = point_return.cartesian[0]
                y = point_return.cartesian[1]
                z = point_return.cartesian[2]
                points.append([x, y, z])
    return points
```

scanner and are able to receive a single frames from it. Among other data such as time or the current scanner configuration, a frame contains a list of scanlines. We iterate over each scanline to obtain each point in a frame. In turn, the Cartesian coordinates of each point are accessible from its point returns, which are configurable to a maximum of 3 in the scanner configuration, but are set to 1 in our case. The list of coordinates then gets saved to the local server in a text file containing the x, y and z components of each point in a new line separated by commas. A complete Python script capable of scheduling scans is included in appendix A.

5.3 Scanner configuration

A suitable time interval between scans is essential to obtain meaningful continuous data and must be considered for each different scanner use case. In our case for continuously monitoring construction progress, selecting a lower time interval is advantageous to follow construction progress from data and have access to on demand up to date scans. However, an increased amount of scans produces more data that must be stored on the local server. Acquiring scans with the Blickfeld Cube 1 Outdoor using the save format of the previously shown software interface results in a file size of up to 10 MB per scan. Not only does more data require additional local storage capacity, remotely accessing and downloading more data for further processing may require an expensive mobile data plan. For the case study, we choose a time interval of 6 hours between scans, which allows us to capture the construction site during and after working shifts.

Configuring the Blickfeld Cube 1 Outdoor's scan pattern impacts its frame rate. An increased number of scanlines lowers the frame rate of the scanner. However, as per

design, the scanner is capable of reaching high frame rates of up to 50 Hz when using a low detail configuration (“Blickfeld”, 2022). As we only scan once every 6 hours, a high frame rate is not required. Therefore, we use the scanner’s maximum amount of 800 scanlines to maximize the point cloud density in each scan. The scanner still reaches a frame rate of 0.7 Hz using maximized scanline settings. As discussed in the simulation, we use the scanner’s highest FOV configuration of 70x30° to maximize the scanned area. Additionally, the angle spacing is set to the lowest possible value of 0.4°. Modifying the scanner’s FOV and angle spacing has no impact on the frame rate.

5.4 Results

Table 5.1: Number of scans acquired each time period in the case study

Time period	Number of scans
02.11.2022 - 09.11.2022	31
15.12.2022 - 13.01.2023	120
07.02.2023 - 16.02.2023	70

In the case study, we continuously collected data in thee time periods, shown in table 5.1. In these time periods, scans were scheduled in 6 hour intervals, resulting in 221 individual scans. In total, scans used 962 MB of drive space, averaging approximately 4.35 MB per scan. Using high detail scanner configurations, each scan consists of up to 82000 points. A fully continuous acquisition of scans could not be achieved due to the power supply of the local hardware setup. Since the power of the hardware setup is connected to the crane, power being cut from the crane stops the acquisition of scans. In the scope of this work, scans showing notable results are picked and further analysed, such as scans showing actual building progress, different areas of the construction site and scans with significant amounts of outliers.

Scans acquired in the case study are generally not aligned in the coordinate system of the BIM, as the scanner rotates with the crane’s top section during operation. Thereby, the scanner acquires the coordinates of points using its local coordinate system, independent of the crane’s rotation, which is unknown to the scanner. As we strictly schedule scans using a time interval of 6 hours, each scan is acquired during an arbitrary crane rotation. For analysis, the point cloud of each selected scan is registered with the BIM to improve visualization and enable comparisons with the BIM. To roughly register point clouds and the BIM, we manually select 4 or more matching points in the BIM and point clouds, which is tedious and time intensive. Applying an ICP algorithm to perform fine registration yields flawed results, since scans from the case study feature a significant amount of outliers that are not related to the BIM. Therefore, we waive further manual processing to remove outliers, since the time intensive effort required to perform a fine registration using ICP is not required for visualization purposes in this work.

5.5 Visual analysis of on-site scans

Scans acquired in the case study show different states and areas of the construction site, depending on when they were acquired and the depending on the crane's rotation. Therefore, we split our analysis in multiple sections, covering notable results collected from reviewing each scan individually, as covering each scan for every state of construction and crane rotation goes beyond the scope of this work. First, we focus on specifically selected scans that mainly cover the construction site in their FOV to discuss the scanned area, identify construction progress, analyse point precision, point cloud density and noise. Additionally, we discuss scans that partly cover the construction site in their FOV and review the impact of the crane's rotation on outliers.

5.5.1 Visually identifying construction progress

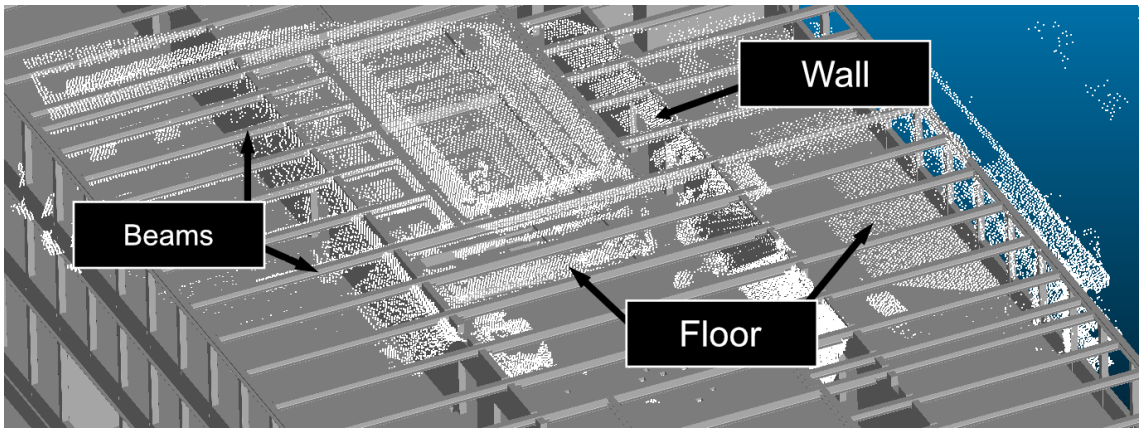

Figure 5.3: Scan overlaid with BIM (02.11.2022-10:10)

First, we focus on scans captured in chronological order that cover the same area around the rectangular recess in the centre of the construction site, shown in fig. 5.4. These scans are specifically selected to show construction progress in a 7 day timespan with similar scanner perspectives due to the acquisition during similar crane rotations. By overlaying the scan shown in fig. 5.4a with the BIM, points corresponding to building elements such as beams, walls and the floor can be identified, as shown in fig. 5.3. Due to limited point precision and errors during the manual registration, some points previously visible in the point cloud without an overlaid BIM in fig. 5.4a can not be seen in fig. 5.3. The next scan captured 2 days later depicts the same area, shown in fig. 5.4b. When comparing the differences of the point clouds from the scans shown in fig. 5.4a and fig. 5.4b, newly built beams spanning horizontally can be identified in bottom region of the latter scan, which are also visible in the BIM. In a scan 5 days later, shown in fig. 5.4c, the partly completed floor of the next storey occluding a large area of the previous storey can be seen. Still, beams, a wall and the floor of the previous storey are partly visible in the bottom right region of the scan, suggesting that the floor of the upper storey has not been completed.

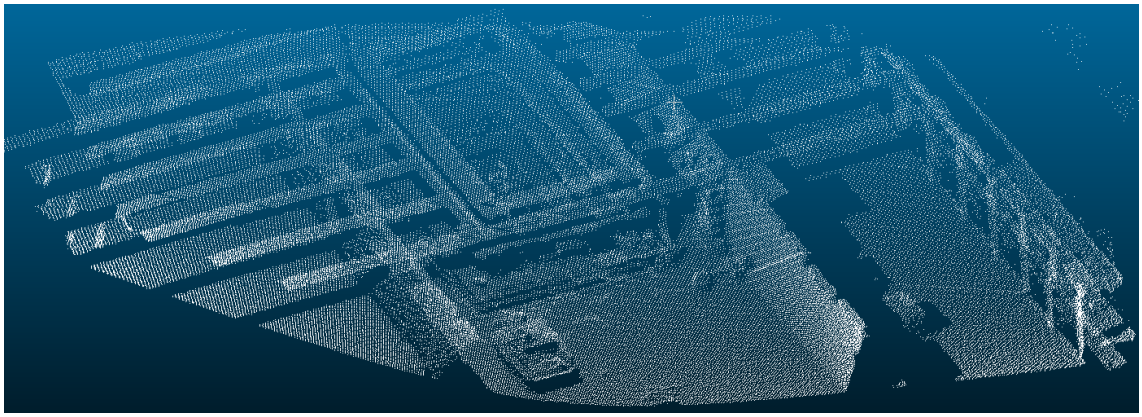

(a) Initial state of construction site (02.11.2022-10:10)

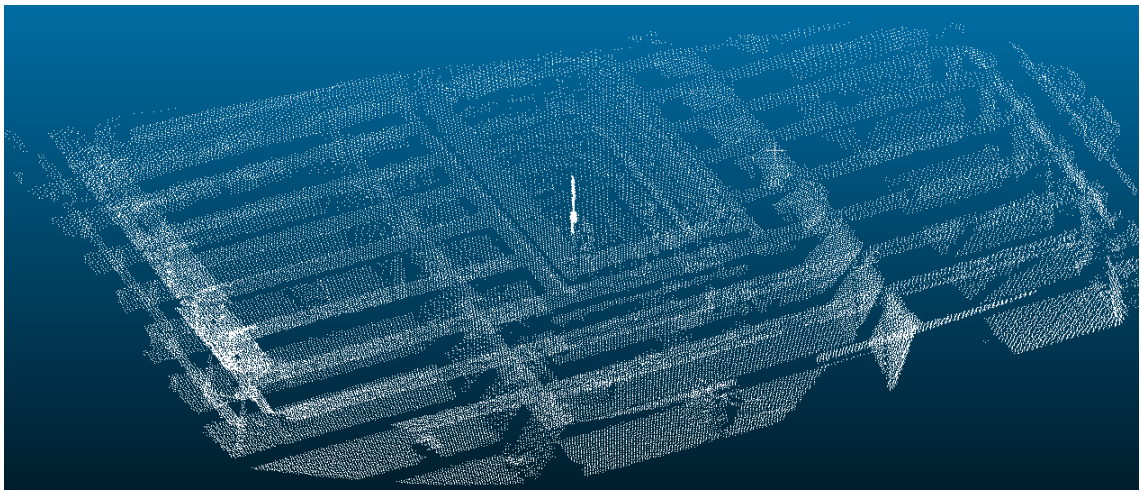

(b) Progressed state of construction site including new beams (04.11.2022-04:14)

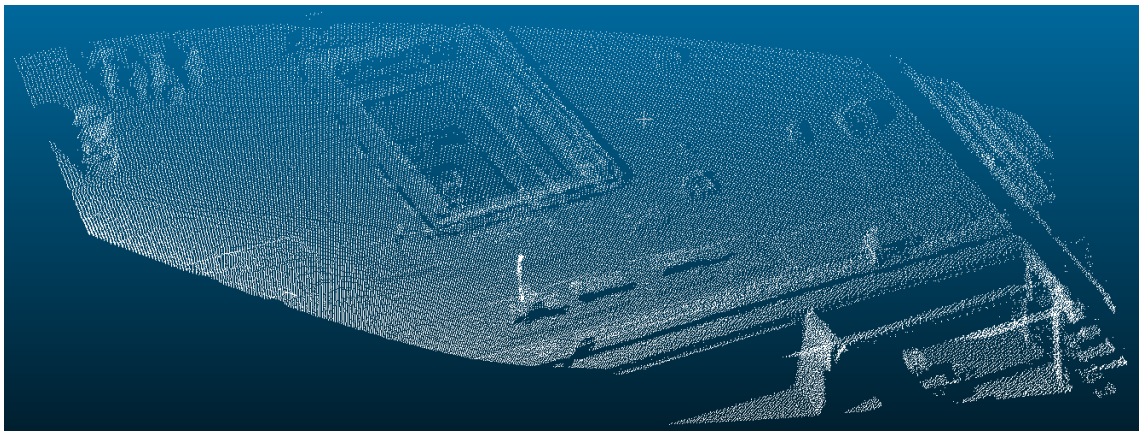

(c) Further progressed state of construction site including partly completed floor (09.11.2022-16:14)

Figure 5.4: Scans in chronological order showing construction progress around a central rectangular recess. Outliers outside of the construction site caused by terrain and adjacent buildings are cropped.

While these scans show the potential to visually identify construction progress, it is important to note that they are specifically picked to show progress. Additional scans between the shown scans exist, but provide limited new information. These scans are either not centred around the rectangular recess due to the crane being rotated differently when the scan was acquired, or there is not visible difference to derive newly build

elements that correspond with the BIM. As such, when identifying construction progress, we are limited to analyse scans with unpredictable viewing directions due to the crane's rotation and can not ensure to monitor specific building elements in succession. Therefore, information on building elements may be missed entirely when a new building element is not captured over longer periods of time and is eventually occluded by following structures. Additionally, it is impossible to determine the order in which elements were built, when changes to multiple building elements occur simultaneously between two successive scans.

5.5.2 Point cloud characteristics

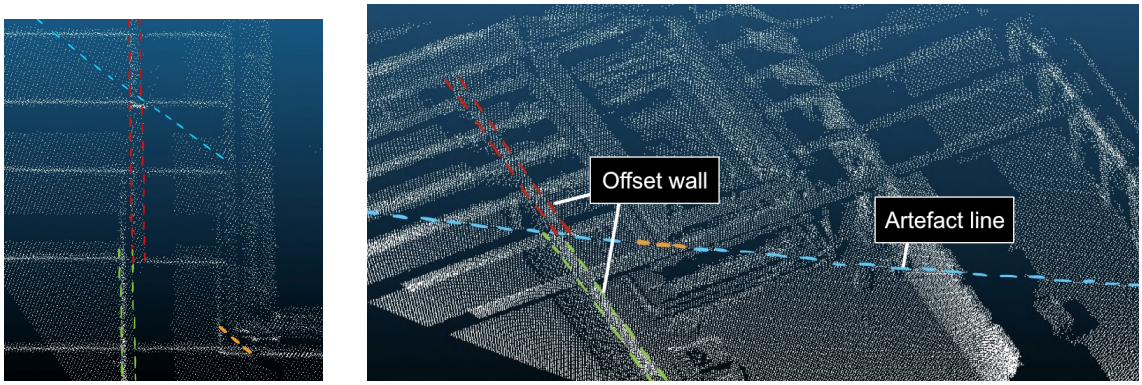

(a) Top-down view (b) Artefact lined up

Figure 5.5: Scanner artefact causing offset walls (02.11.2022-10:10)

While building elements generally line up and correspond with the BIM after manual registration, the accuracy of point clouds is limited by a horizontal phase offset caused by the scanner hardware. Therefore, all scans acquired using the Blickfeld Cube 1 Outdoor in the case study are shifted horizontally above and blow the scanner's local horizon. Any building element along the local horizon of the scanner appears cut diagonally when using the scanner with a downwards pitch, shown in fig. 5.5 The offset in this point cloud can especially be seen along a wall in a top-down view in fig. 5.5a, highlighted in red and green above and below the scanner's local horizon, which is highlighted in blue and orange. Generally, the scanner artefact can be fixed manually by iteratively adjusting an offset passed by using the Blickfeld Python library ("Release v1.21", n.d.). However, as our data was acquired before knowing the existence of this artefact and iterative solution, point clouds from the case study can not retroactively be fixed.

Scans in the case study are affected by noise, which is especially visible on flat surfaces. When viewing points depicting flat surfaces in a cross section, a blurry line of points can be seen, while the cross section of a flat surface in a point cloud with no noise should show a straight line. In the scope of this work, we perform a point cloud to mesh distance measurement for a floor segment, to determine the order of magnitude of noise for one example. For this measurement, we choose a supposedly flat floor surface from a point cloud segment with no outliers. The floor segment is cut out of the original point cloud

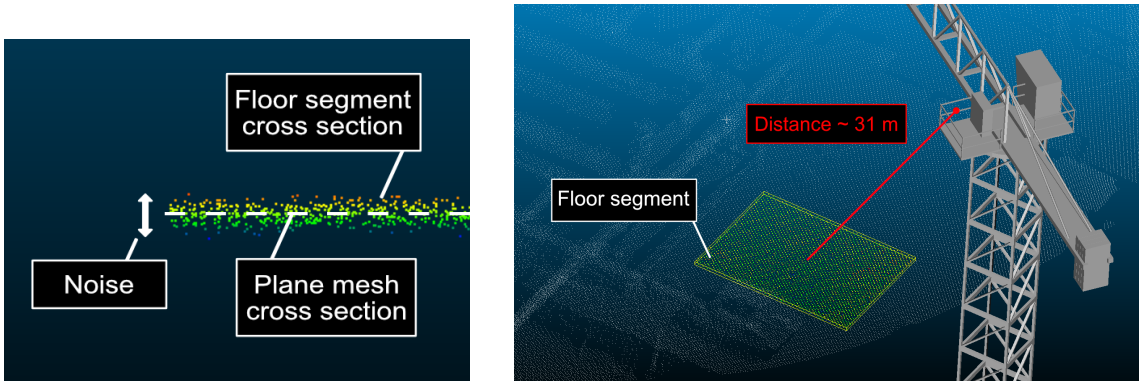

(a) Cross section of floor point cloud segment with a matched plane mesh

(b) Distance from crane to floor point cloud segment

Figure 5.6: Setup to measure distance from floor point cloud segment to plane mesh (02.11.2022-10:10)

and a plane mesh is aligned along the approximate centre of the points making up the floor segment, shown in fig. 5.6a. However, due to registration inaccuracies, the actual location of the floor mesh is unknown. Therefore, we assume that the actual floor is in the centre of the point cloud segment for the point cloud to mesh distance measurement. The results show an unsigned mean distance from the plane mesh to any point of 1.50 cm with a standard deviation of 1.14 cm for a distances of approximately 31 m from the scanner.

The Blickfeld Cube 1 Outdoor has a range precision of less than 2 cm for targets with a distance of 10 m and 50% reflectivity, according to the datasheet of the scanner (“Blickfeld”, 2022). We however use the scanner mounted on a crane while pitched downwards, easily exceeding ranges of 10 m and therefore observe more noise in our scans. Another possible cause for inaccurate points is movement of the scanner during a scan. Crane rotation, wind and heavy crane loads are plausible causes for scanner movement relative to the construction site. However, as we run the scanner using a high frame rate of 0.7 Hz, a scan only requires approximately 1.42 s to complete, resulting in a short time period during which the scanner is prone to movement. Therefore, it appears likely that inaccurate points are a result of the scanner’s precision limitations.

Another limitation of scanning the construction site from a crane is the point cloud density. In our case, the scanner is configured to use a 0.4 ° angle spacing between points on a scanline. Naturally, the point spacing increases for distant points from the scanner using a constant angle spacing. We manually measure distances between points in the point cloud shown in fig. 5.4a, to show the order of magnitude for point spacing. Generally, we can measure distances between points in a range of 5 to 10 cm for distances of approximately 25 m from the scanner. For distances of approximately 50 m from the scanner, we can measure distances of up to 30 cm between points.

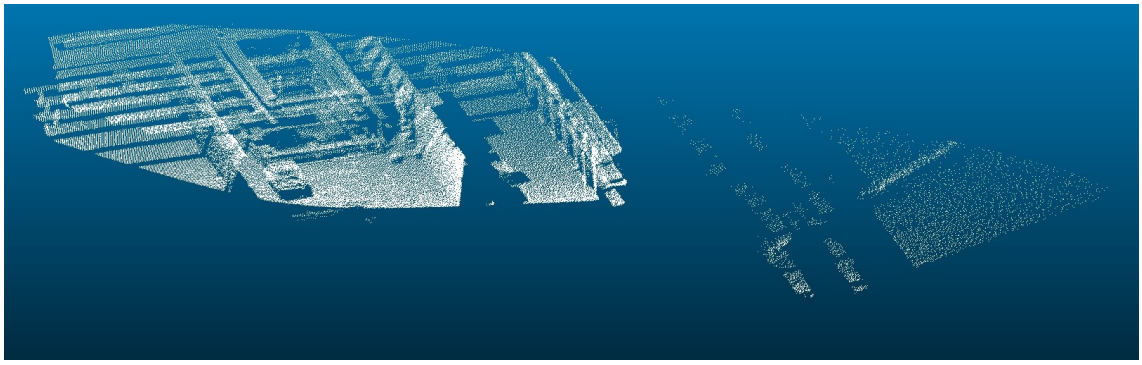

Figure 5.7: Complete point cloud of previously cropped fig. 5.4a, showing outliers on the right side (02.11.2022-10:10)

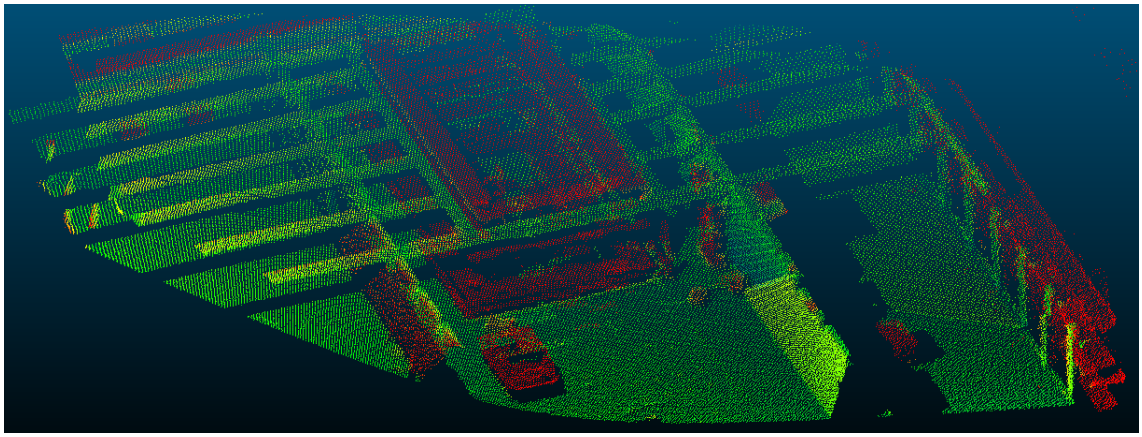

Figure 5.8: Point cloud coloured in a gradient from green (0 cm) to red (>50 cm) depending on point distances to the BIM (02.11.2022-10:10)

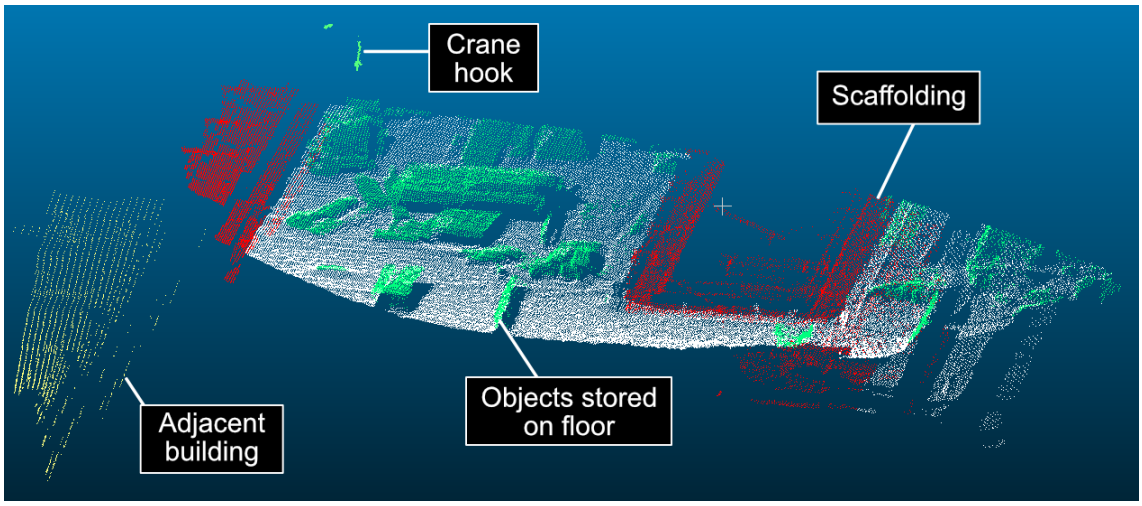

Figure 5.9: Manually segmented point cloud showing the different causes of outliers (17.12.2022-03:56)

5.5.3 Outliers

In the scope of this work, we define outliers as points that do not correspond with any building element of the BIM after registration. Scans in our case study feature a significant amount of outliers in close and distant proximity to the BIM for registered point clouds.

Outliers distant to the BIM, as seen on the right side of fig. 5.7, which shows all points of the previously cropped point cloud in fig. 5.4a, are mostly caused by terrain and adjacent buildings. The amount of outliers caused by terrain and adjacent buildings depends on how much of the scanner's FOV covers the construction site. In addition, scans feature outliers in closer proximity to the BIM. This is shown in fig. 5.8, which depicts a point cloud coloured in a gradient from green to red. Depending on the nearest distance from each point to the BIM, it is coloured from green (0 cm) to red (>50 cm). As the distance to the BIM depends on the precision of the manual registration, the accuracy of this gradient is limited. However, using the color gradient, it is possible to visually interpret outliers close to the BIM. For example, the red points around the rectangular recess in the centre of the scan and on the right border of the building, outside of the BIM, suggest to be scaffolding. Additionally the offset by the scanner artefact causing the horizontal offset in the left wall can be seen, as the wall in the lower region of the artefact line is further distant to the BIM than the wall matching the registration above the artefact.

A manually segmented scan that further points out outliers is shown in fig. 5.9. This scan shows the floor of the left side of the rectangular recess with a significant amount of outliers on top. While a manual segmentation leaves room for speculation when classifying outliers, we make an educated guess using knowledge of the construction site, the building's geometry and surroundings for our case study. Red points are mapped to scaffolding, green points are mapped to any objects stored on the floor and the crane's hook located above the building and yellow points are mapped to terrain and an adjacent building on the left side. The remaining white points belong to building elements in the BIM, which is only the floor in this case.

5.5.4 Impact of crane rotation on scanned area

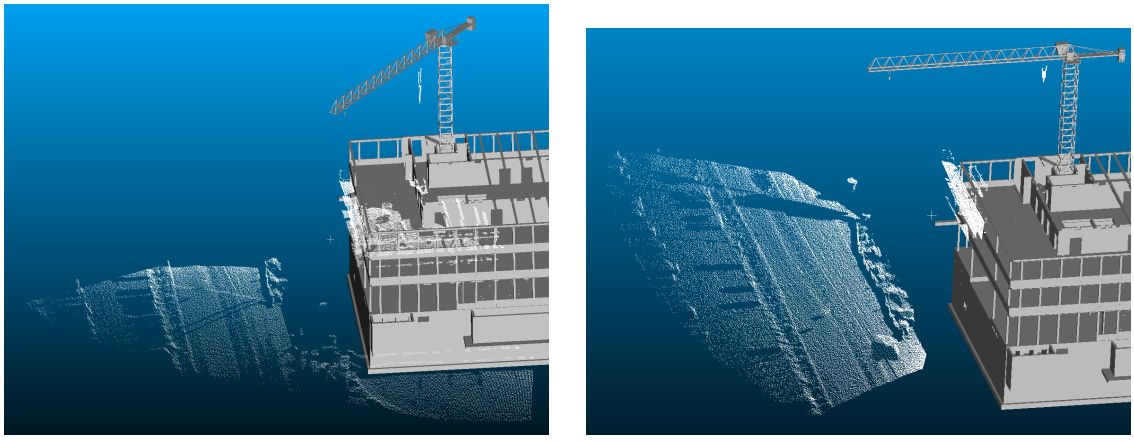

(a) Partly covered building (02.11.2022-16:14)

(b) No coverage of building (02.11.2022-22:14)

Figure 5.10: Coverage of the building for crane rotations facing away from centre of construction site

As previously discussed, distant objects outside of the construction site in the scanner's FOV are also captured. Due to partial coverage of the construction site caused by unpredictable crane rotation when scheduling scans by a fixed time interval, some scans

show a significant amount of distant outliers. To illustrate the amount of points depicting distant outliers that correspond to terrain or an adjacent building, two exemplary scans are overlaid with the BIM in fig. 5.10. Additionally, the crane rotation during the acquisition of each scan in the figures is visualised using a crane model. We can observe that the scan in fig. 5.10a shows partly coverage in a corner area of the building, while a significant amount of points lay outside of the building depicting an adjacent street. A more extreme example is shown in fig. 5.10b, where the scanner does not cover the building at all. As such, it is barely possible to perform manual registration due to the lack of reference points with the BIM. Therefore, scans performed with crane rotations facing away from the centre of the construction site barely provide information on building elements and mostly capture outliers.

5.5.5 Long term results

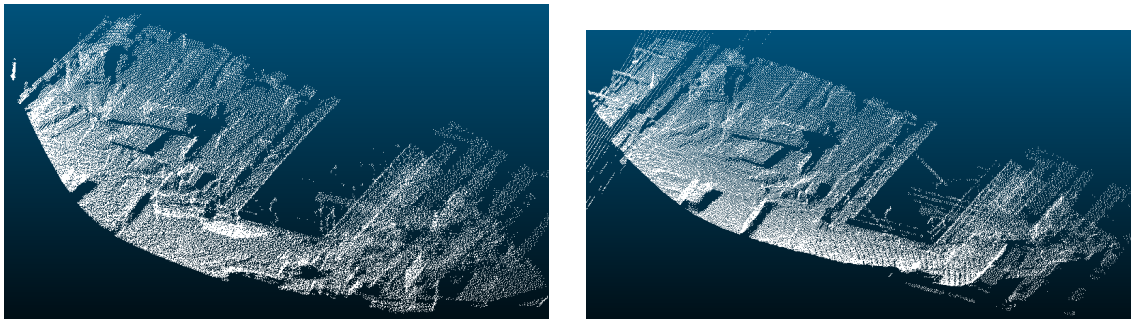

(a) Start (17.12.2022-03:56) (b) End (09.01.2023-03:56)

Figure 5.11: Point clouds of construction site in the beginning (left) and end (right) of a 24 day timespan with no visible changes

Apart from analysing scans individually, different long term trends in the context of construction progress can be observed. First, there is no visible change in construction progress for any scan in a 24 day timespan between 17.12.2022 and 09.01.2023. Scans in this timespan show the same area of the construction site with insignificant changes in crane rotation, which are presumably caused by wind. Scans at the start and end of the 24 day timespan, shown in fig. 5.11, and all scans in between cover the same area of the construction site. This break in construction progress can be confirmed in the construction schedule, which suggests that work might be obstructed by weather in this specific timespan, where we observe no changes in our scans.

Additionally, we can observe multiple scans in succession that have a limited view to most areas of the building. In particular, 9 scans from 07.11.2022 to 09.11.2022 do not cover any area to the right of the rectangular recess at all. Instead, a significant amount of the scanner's FOV covers adjacent buildings or terrain, shown in fig. 5.12. To visualize the lack of coverage on the right side of the rectangular recess, the scans are overlaid in with the BIM in fig. 5.12. All areas covered in the timespan of 9 scans can be identified by point clouds coloured in white. The green point cloud shows the first scan after the 9 scans coloured in white, which covers the right side of the rectangular recess. Scans in this

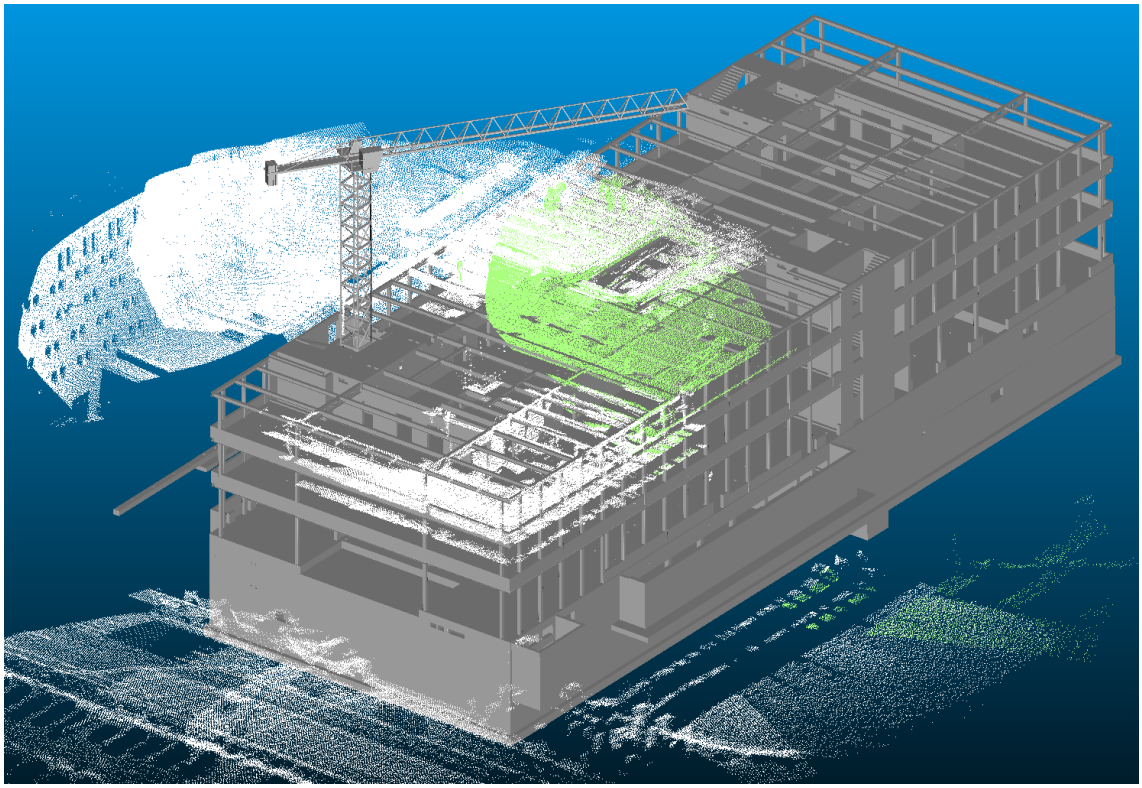

Figure 5.12: Point clouds in timespan between 07.11.2022-10:14 and 09.11.2022-16:14 overlaid with BIM showing scanned areas. The last scan is coloured green

timespan are not only barely covering the construction site and produce significant amount of outliers, but there are no scans monitoring progress on any area that is not coloured in white, limiting the ability to derive construction site progress continuously.

Chapter 6

Discussion

Using the 221 scans acquired in the case study, the scanner placement and configuration can be reviewed. Apart from limitations specific to scanner properties, such as FOV, angle spacing, precision or artefacts, scans acquired in the case study are limited in capturing similar areas on the construction site reliably, due to the fixed scan schedule. As previously discussed in section 5.5.4 focusing on scans that only partly capture the construction site, a rotating crane combined with scheduling scans purely based on a fixed time interval limits the ability to capture predictable areas of the construction site continuously. Therefore, scanned areas may include specific regions the construction site by chance, but may also cover a significant region outside of the constructions site, producing outliers unrelated to the construction site.

The inability to ensure scans covering specific regions on the constructions site, resulting in successive scans capturing potentially useless regions for construction monitoring, suggests changes to the scanner position or scan schedule. By scheduling scans with a decreased time interval, the chance to capture a specific area on the construction site can be increased, when the scanner is mounted on a rotating crane. However, relying on an increased amount of scans does not guarantee coverage of a specific area. In cases when the crane is not used for an extended time period while facing away from regions to monitor, the coverage of scans is limited to the direction of the crane. Similarly, in cases in when construction work requires the crane for one region of the construction site over an extended amount of time, coverage on other areas that progress without requiring the crane is not ensured. As previously shown in fig. 5.12 in a time period of 2 days, crane rotations facing away from the building cause successive scans capturing an adjacent building. It is unclear, whether a decreased scan interval would allow acquisition of scans when the crane is facing towards the centre of the constructions site, since its rotation is still unknown to the scanner and there is no information when and towards which direction the crane rotates. Therefore, the captured area and building elements inside of it are unpredictable when implementing a decreased scan interval and can not ensure to capture a specific area of the construction site. Additionally, a lower scan interval further increases data volume and processing efforts, which may already require significant effort due to the coverage of unpredictable outliers.

Therefore, a compromise using the scanner mounted at a non rotating position on the crane may be advantageous in practice. The main disadvantage using a non rotating scanner position is the limited area covered by the scanner. However, opposed to a rotating scanner position covering different areas in each scan, the area is fixed after the scanner setup, allowing for reliable coverage of specific regions, independent of the crane's rotation. As such, registration of acquired point clouds may be eased, depending on how the

Table 6.1: Comparison of fixed and rotating scanner positions on a crane

Scanner position on crane	Tower (non rotating)	Jib (rotating with crane)
Size of covered area	Limited by scanner position and FOV	Any areas in scanner's FOV reachable with crane's rotation
Registration	Similar transformation matrices	Different transformation matrices depending on crane rotation
Position variety	Limited to any position on crane's tower	Limited to elevated positions near the cabin and the crane's jib
Reliability to capture specific area	Fixed in scanner FOV after setup	Unpredictable

scanner orients point clouds in its internal coordinate system for successive scans. Using the Blickfeld Cube 1 Outdoor, running scans with a similar scanner orientation leads to similarly oriented point clouds, allowing coarse registration with the BIM by applying similar transformation matrices to point clouds. This is not the case for a rotating scanner position, requiring different transformation matrices, which are unknown since our hardware setup has no information of the crane's rotation. Additionally, non rotating scanner positions on cranes are only available on the crane's tower. Therefore, scanner positions on the crane's jib allowing different scanner orientations and views onto the construction site, such as scanning straight downwards, are not available. Furthermore, as previously shown in the simulation in fig. 4.7b, a fixed scanner position on the crane's tower below the rotating top section still covers a similarly sized area of the constructions site compared to a rotating scanner position slightly higher next to the cabin, in regard to a single scan. A comparison between using a rotating and non rotating scanner position on a crane is shown in table 6.1.

Point clouds generated in the simulation generally line up with real world scans, despite using a TLS based scan pattern, which differs from the Blickfeld Cube 1 Outdoor's scan pattern. Therefore, the size and shape of point clouds is different in the simulation and case study, despite using the same scanner FOV in the simulation and case study. Real world scans acquired with the Blickfeld Cube 1 Outdoor are generally wider horizontally than in the simulation. A direct comparison regarding the covered area and occlusions is limited by the real scanner's pitch angle, which was not accurately set up in the case study, causing deviations from an exact downwards pitch of 45°. In addition, the simulation is limited by its inability to replicate noise and outliers. An accurate simulation replicating the scan pattern of the Blickfeld Cube 1 Outdoor is advantageous when an accurate prediction of the coverage of larger regions of the constructions site is required. Especially when using a fixed scanner position for sophisticated construction sites, the limited scanner FOV may not be sufficient to capture larger or multiple areas around the construction site. Therefore, an accurate simulation of the scanned area is advantageous in order to

accurately plan coverage and the required number of scanners in advance, before setting them up on the real construction site.

Additionally, our results are limited to the shape of the constructions site from the case study. As the building mostly consists of large rooms and corridors parallel to the scanner's view direction, when facing towards the central rectangular recess, there are few occlusions caused by building elements, such as walls. It remains unclear, whether occlusions on more sophisticated building layouts have a significant effect on scans acquired from cranes. The limited point cloud density for distant objects observed in section 5.5.2 limits the ability to derive accurate shapes from points. Additionally, the use of a single scanner only enables coverage of building elements from one side. As such, the LIDAR sensor in this work seems insufficient for detailed area or volume calculations of individual building elements when scanning from cranes. To increase the point cloud density using the same scanner, the distance from the scanner to the building must be smaller. However, a smaller distance results in a decrease of the scanned area, as observed in the simulation. The results are promising in the context of Scan-vs-BIM use cases, since the precision of the scanner produces a limited amount noise. Therefore, a separation of points caused by noise and points which are outliers by a comparison with the BIM is eased. As previously shown in fig. 5.8, a coarse manual registration with the BIM is sufficient to visually separate points belonging to building elements and outliers. This is promising for Scan-vs-BIM use cases, where low threshold values enabled by a limited amount of noise may be required. In general, the LIDAR sensor used in the case study shows potential as a technology to acquire 3D point cloud data on cranes for continuous monitoring.

Chapter 7

Conclusion

In this work, we discuss the viability of using LIDAR sensors mounted on cranes for continuous construction monitoring. We present an alternative approach to acquire 3D point cloud data on construction sites, compared to commonly implemented approaches in research using TLS or image construction. Our approach is split into a simulation and case study, carried out using the Blickfeld Cube 1 Outdoor LIDAR sensor on a real construction with an available BIM. By simulating the scanner from different positions on a crane using a simplified approach only focusing on FOV and occlusions, we are able to determine a suitable scanner position that can be used on the real construction site to maximize the covered area from the scanner. In the case study, the scanner is added to an existing hardware setup on the crane, which provides data storage, remote access and the ability to acquire continuous scans by a fixed time interval.

Running the scanner for multiple time periods in the case study, we successfully acquire 221 scans for further analysis. It is possible to visually derive progress of building elements from differences in successive scans acquired from the crane by comparing point clouds with a BIM. However, due to the scanner's position rotating with crane and scan scheduling by a fixed time interval, we are not able to acquire continuous scans of specific regions of the construction site consistently. To effectively implement LIDAR scanners on cranes in construction, a compromise between the scanner's position on the crane, limiting the covered area and the time interval limiting the consistency of capturing a specific area of the construction site is needed.

In future research, we suggest to focus on using multiple non rotating scanner positions, enabling consistent acquisition of scans with an increased area covering the construction site from different perspectives. This requires a reworked scan scheduling approach implementing synchronization of multiple scanners. In addition, an advanced simulation able to accurately replicate LIDAR scanner properties in different orientations is needed to effectively plan the positions of multiple scanners before deploying them on a construction site.

Appendix A

Digital appendix

The digital appendix includes:

- animated versions (.gif) of selected figures to improve visualization of point clouds
- files implementing the simulation
- simulated point clouds
- Python script and library requirements to schedule scans with the Blickfeld Cube 1 Outdoor
- scans acquired in case study
- collection of manually registered scans from the case study

Bibliography

Blenderbim [Accessed: 03.02.2023]. (n.d.). https://blenderbim.org/

Blickfeld [Accessed: 02.02.2023]. (2022). https://www.blickfeld.com/lidar-sensor-products/cube-1/

Blickfeld. (2023). Blickfeld-scanner-lib [Accessed: 22.02.2023]. https://github.com/Blickfeld/blickfeld-scanner-lib

Borrmann, A., König, M., Koch, C., & Beetz, J. (2018). *Building information modeling : Technology foundations and industry practice*. Springer International Publishing AG.

Braun, A., Tuttas, S., Borrmann, A., & Stilla, U. (2020). Improving progress monitoring by fusing point clouds, semantic data and computer vision. *Automation in Construction*, *116*. https://doi.org/10.1016/j.autcon.2020.103210

Collins, F., Pfitzner, F., & Schlenger, J. (2022). Scalable construction monitoring for an as-performed progress documentation across time. *Proceedings of 33. Forum Bauinformatik*.

Dore, C., & Murphy, M. (2014). Semi-automatic generation of as-built bim façade geometry from laser and image data. *Journal of Information Technology in Construction ITCON*, *ITcon Vol. 19, pg. 20-46, http://www.itcon.org/2014/2*, 20–46.

Golparvar-Fard, M., Peña-Mora, F., & Savarese, S. (2015). Automated progress monitoring using unordered daily construction photographs and ifc-based building information models. *Journal of Computing in Civil Engineering*, *29*(1), 04014025. https://doi.org/10.1061/(ASCE)CP.1943-5487.0000205

Han, K. K., & Golparvar-Fard, M. (2017). Potential of big visual data and building information modeling for construction performance analytics: An exploratory study. *Automation in Construction*, *73*, 184–198. https://doi.org/https://doi.org/10.1016/j.autcon.2016.11.004

Holst, C., Kuhlmann, H., Paffenholz, J.-A., & Neumann, I. (2015). Tls im statischen, stop & go sowie kinematischen einsatz.

Jiang, Z., Shen, X., Ibrahimkhil, M., Barati, K., & Linke, J. (2022). Scan-vs-bim for real-time progress monitoring of bridge construction project. *ISPRS Annals of the Photogrammetry, Remote Sensing and Spatial Information Sciences*, *X-4/W3-2022*, 97–104. https://doi.org/10.5194/isprs-annals-X-4-W3-2022-97-2022

Kavaliauskas, P., Fernandez, J. B., McGuinness, K., & Jurelionis, A. (2022). Automation of construction progress monitoring by integrating 3d point cloud data with an ifc-based bim model. *Buildings*, *12*(10). https://doi.org/10.3390/buildings12101754

Liu, J., Xu, D., Hyyppä, J., & Liang, Y. (2021). A survey of applications with combined bim and 3d laser scanning in the life cycle of buildings. *IEEE Journal of Selected Topics in Applied Earth Observations and Remote Sensing*, *14*, 5627–5637. https://doi.org/10.1109/JSTARS.2021.3068796

Omar, T., & Nehdi, M. L. (2016). Data acquisition technologies for construction progress tracking. *Automation in Construction*, *70*, 143–155. https://doi.org/https://doi.org/10.1016/j.autcon.2016.06.016

Pučko, Z., Šuman, N., & Rebolj, D. (2018). Automated continuous construction progress monitoring using multiple workplace real time 3d scans. *Advanced Engineering Informatics*, *38*, 27–40. https://doi.org/https://doi.org/10.1016/j.aei.2018.06.001

Raj, T., Hashim, F. H., Huddin, A. B., Ibrahim, M. F., & Hussain, A. (2020). A survey on lidar scanning mechanisms. *Electronics*, *9*(5). https://doi.org/10.3390/electronics9050741

Release v1.21 [Accessed: 08.03.2023]. (n.d.). https://docs.blickfeld.com/cube/latest/firmware/doc/release_notes/v1.21/public.html?highlight=offset#adjustment-possibility-for-horizontal-phase-offset-v1-21-1

Sacks, R., Brilakis, I., Pikas, E., Xie, H. S., & Girolami, M. (2020). Construction with digital twin information systems. *Data-Centric Engineering*, *1*, e14. https://doi.org/10.1017/dce.2020.16

Scan pattern [Accessed: 02.02.2023]. (n.d.). https://docs.blickfeld.com/cube/latest/scan_pattern.html

Tang, X., Wang, M., Wang, Q., Guo, J., & Zhang, J. (2022). Benefits of terrestrial laser scanning for construction qa/qc: A time and cost analysis. *Journal of Management in Engineering*, *38*(2), 05022001. https://doi.org/10.1061/(ASCE)ME.1943-5479.0001012

Winiwarter, L., Esmorís Pena, A. M., Weiser, H., Anders, K., Martínez Sánchez, J., Searle, M., & Höfle, B. (2022). Virtual laser scanning with helios++: A novel take on ray tracing-based simulation of topographic full-waveform 3d laser scanning. *Remote Sensing of Environment*, *269*. https://doi.org/https://doi.org/10.1016/j.rse.2021.112772

Wu, C., Yuan, Y., Tang, Y., & Tian, B. (2022). Application of terrestrial laser scanning (tls) in the architecture, engineering and construction (aec) industry. *Sensors*, *22*(1). https://doi.org/10.3390/s22010265

Xu, S., Wang, J., Shou, W., Ngo, T., Sadick, A.-M., & Wang, X. (2021). Computer vision techniques in construction: A critical review. *Archives of Computational Methods in Engineering*, *28*(5), 3383–3397. https://doi.org/10.1007/s11831-020-09504-3

Xue, J., Hou, X., & Zeng, Y. (2021). Review of image-based 3d reconstruction of building for automated construction progress monitoring. *Applied Sciences*, *11*(17). https://doi.org/10.3390/app11177840

Declaration

I hereby affirm that I have independently written the thesis submitted by me and have not used any sources or aids other than those indicated.

München, 16.03.2023 

Location, Date, Signature